

# Integrated causal-predictive machine learning models for tropical cyclone epidemiology

Rachel C. Nethery<sup>1</sup>, Nina Katz-Christy<sup>2</sup>, Marianthi-Anna Kioumourtzoglou<sup>3</sup>,  
Robbie M. Parks<sup>3</sup>, Andrea Schumacher<sup>4</sup>, G. Brooke Anderson<sup>5</sup>

<sup>1</sup>Department of Biostatistics, Harvard T.H. Chan School of Public Health

<sup>2</sup>Department of Statistics, Harvard University, Faculty of Arts and Sciences

<sup>3</sup>Department of Environmental Health Sciences, Columbia Mailman School of Public Health

<sup>4</sup>Cooperative Institute for Research in the Atmosphere, Colorado State University

<sup>5</sup>Department of Environmental & Radiological Health Sciences, Colorado State University

## Abstract

Strategic preparedness has been shown to reduce the adverse health impacts of hurricanes and tropical storms, referred to collectively as tropical cyclones (TCs), but its protective impact could be enhanced by a more comprehensive and rigorous characterization of TC epidemiology. To generate the insights and tools necessary for high-precision TC preparedness, we develop and apply a novel Bayesian machine learning approach that standardizes estimation of historic TC health impacts, discovers common patterns and sources of heterogeneity in those health impacts, and enables identification of communities at highest health risk for future TCs. The model integrates (1) a causal inference component to quantify the immediate health impacts of recent historic TCs at high spatial resolution and (2) a predictive component that captures how TC meteorological features and socioeconomic/demographic characteristics of impacted communities are associated with health impacts. We apply it to a rich data platform containing detailed historic TC exposure information and Medicare claims data. The health outcomes used in our analyses are all-cause mortality and cardiovascular- and respiratory-related hospitalizations. We report a high degree of heterogeneity in the acute health impacts of historic TCs at both the TC level and the community level, with substantial increases in respiratory hospitalizations, on average, during a two-week period surrounding TCs. TC sustained windspeeds are found to be the primary driver of increased mortality and respiratory risk. Our modeling approach has broader utility for predicting the health impacts of many types of extreme climate events.

## 1 Introduction

The US National Oceanic and Atmospheric Administration reports that tropical cyclones (TCs) impose the largest financial burden of any weather disasters in the US, costing \$945.9 billion since 1980 or roughly \$21.5 billion per event (National Oceanic and Atmospheric Administration, 2020). TCs, which include hurricanes and tropical storms, often bring severe winds, rainfall, and flooding (Shultz et al., 2005), which can catalyze massive property and infrastructure damage. Due to the diverse types of hardships that can be set in motion by TC, the full spectrum of human health impacts of TCs are incompletely understood and unreliably quantified. Extreme weather events are known to cause both “direct” and “indirect” health impacts. It is well-appreciated that TCs introduce severe risks for accidental mortality and injuries (Centers for Disease Control and Prevention, 2005; Rappaport, 2014; Rappaport and Blanchard, 2016; Gong et al., 2007), such as drowning or blunt force trauma from falling debris, which are known as “direct” health impacts, as they are straightforwardly attributed to the TC (i.e., the causal mechanism has been clearly identified). Direct TC health impacts are generally the focus of post-storm surveillance in the US.

TCs can also “indirectly” elevate risk for a range of other adverse health events because, for example, they often cause power outages (Chen et al., 2018; Han et al., 2009; Klinger and Owen Landeg, 2014;

Lane et al., 2013; Sanchez, 2017; Shultz and Galea, 2017), trigger mass evacuations (Lew and Wetli, 1996; Brunkard et al., 2008; Centers for Disease Control and Prevention, 2013; Dosa et al., 2012), create psychological stress (Lutgendorf et al., 1995; Lenane et al., 2017), require clean-up (Centers for Disease Control and Prevention, 2004; Lew and Wetli, 1996), increase exposure to heat and pollution (Shultz and Galea, 2017), and interfere with normal medical care and medication use (Klinger and Owen Landeg, 2014; Gray and Hebert, 2007). Post-storm surveillance can hugely underestimate these indirect health impacts of TCs, as evidenced by Hurricane Maria. While surveillance initially attributed 64 deaths in Puerto Rico to the storm (BBC, 2018), later epidemiological studies estimated that the storm caused >2,000 deaths (Kishore et al., 2018; Santos-Burgoa et al., 2018; Rivera and Rolke, 2018; Santos-Lozada and Howard, 2018; BBC, 2018).

The literature on TC epidemiology has been dominated by single-storm studies (Sharma et al., 2008; McQuade et al., 2018; Gotanda et al., 2015; Swerdel et al., 2014; Greenstein et al., 2016; Kim et al., 2016), seeking to quantify the total excess mortality or morbidity caused by a TC (including both direct and indirect effects). This focus on single storms was driven by widespread acknowledgement of substantial heterogeneity in TC health impacts. Recently, the first large-scale study was conducted to estimate average health effects across all TCs impacting the US over a 12-year period (Yan et al., 2020). While these studies have helped to reveal fundamental features of TC epidemiology, the results of single-storm studies may not generalize well, and multi-storm average health effects are too coarse to explain across-storm variability. Thus these studies have been unable deliver the targeted yet generalizable insights needed to guide strategic storm preparedness, which is believed to be one of the most effective tactics for minimizing TC health impacts (Thomalla and Schmuck, 2004; Shultz et al., 2005; Keim, 2008). A 2020 report by the National Academies of Sciences, Engineering, and Medicine stressed that in order to strengthen disaster resilience, improve responses, and quicken recoveries, the US needs a uniform approach to quantifying disaster-related mortality and morbidity, as well as new analytical methods to enable estimation of disaster health impacts and the capacity to implement such methods on population-level data (National Academies of Sciences, Engineering, and Medicine, 2020).

The goal of our work is to inform strategic TC preparedness through development and application of a new modeling approach that (1) standardizes estimation of acute health impacts across past TCs, (2) discovers common patterns and sources of heterogeneity in those health impacts, and (3) enables identification of communities at highest health risk for future TCs. First, the proposed approach must incorporate a causal inference component that, when applied to historic data, estimates the excess adverse health events caused by past TCs (hereafter “health effects” or “health impacts”) at high spatial resolution in a standardized and transparent fashion. These estimates should capture both direct and indirect effects and should be adjusted for confounding. A TC’s health impact in a particular community may be influenced (i.e., modified) by a complex interplay among the features of the storm and the population (Keim, 2008), and understanding these drivers of heterogeneity is a key aim of our work. Thus, the second component of our approach is a predictive model relating the community- and TC-specific health impacts to the TC’s meteorological features and the socioeconomic/demographic features of the community. In addition to offering unprecedented insights into multi-storm TC epidemiology, this approach allows for community-specific prediction of the health impacts of an approaching TC with forecasted track and features. The predictive model could also be used to create general community-level TC health risk profiles based on a collection of representative future TC exposures. This tool represents a first step toward identifying communities at highest risk for adverse TC health impacts so that they can be targeted for immediate TC strategic preparedness and/or long-term efforts to increase resilience.

Building on a rich dataset of recent historic US TC exposures and Medicare claims, we introduce an innovative statistical modeling approach that incorporates both the causal inference and predictive components described above. Our Bayesian machine learning method jointly fits causal inference sub-models to estimate the county-specific health effects of each historic TC, then passes these effect estimates into a predictive sub-model that captures relationships between county and TC features and health impacts. Leveraging recent advances in causal inference with observational pre/post treatment data, the causal sub-

models employ a matrix completion approach that adjusts for unmeasured, time-varying confounding under mild assumptions (Athey et al., 2018). By joining the causal and predictive models in a Bayesian framework, we account for the uncertainty from all components, and predictions made using this model are accompanied by accurate uncertainty estimates, which are critical to assess their utility. This method can be widely used for characterizing and predicting the health impacts of extreme weather and climate events.

## 2 Methods

### 2.1 Data

The data and the study design are described only briefly here, detailed descriptions and justifications of these choices are provided in Section S.1. All mortalities, respiratory disease hospitalizations, chronic obstructive pulmonary disease (COPD) hospitalizations, and cardiovascular disease (CVD) hospitalizations in the Medicare population are obtained for the period 1999–2015. Using detailed track and meteorologic data for all Atlantic-basin TCs during the same period, we classify counties as exposed (equivalently “treated” for consistency with the causal inference literature) or controls for each TC. Counties that experience TC maximum sustained windspeeds of gale force or higher ( $\geq 17.4$  meters/second) at the population mean center are considered treated, and untreated counties within 150 miles of a treated county are eligible to serve as controls. Additional inclusion criteria to prevent modeling instability are applied to determine the final set of analytic treated and control counties for each TC (Section S.1.3).

For each treated and control county, we extract a time series of two-week cumulative counts of a given health outcome (e.g. mortality) for a 140-day period starting 129 days prior to the TC’s first US approach and ending 11 days after. We use these time series to construct a (separate) panel data matrix for each TC and outcome, the general structure of which is illustrated in Figure 1A. While the figure is intentionally left general, in our context only the final two-week window in the time series (the final column in the matrix) is considered to be the “treatment period” for treated counties. This corresponds to a two-week period beginning 2 days prior to the TC’s arrival and ending 11 days after (Yan et al., 2020). For the predictive component of our model, we also obtain county-specific TC features (e.g., maximum sustained windspeed, duration of sustained wind speeds above 20 m/s) and socioeconomic and demographic characteristics for each TC and each exposed county.

### 2.2 Approach

For each health outcome, we construct a model composed of (1) causal inference sub-models for each TC to estimate the excess health events attributable to it in each impacted county and (2) a predictive sub-model that relates these health effects to the TC and county features. We emphasize that each health outcome is modeled separately, with no transfer of information between the outcome-specific models. For the remainder of the section, we focus on the model for a single outcome. To emphasize the broader applicability of our approach, we present the methods using general notation, making connections back to our specific TC data structures for clarity.

#### 2.2.1 Causal inference sub-models

In this section, we describe the models that will be used to estimate the excess health events attributable to historic TCs. These models are applied separately to the data for each TC, which is part of a larger modularized model fitting scheme described in Section 2.2.2.

We denote the number of TCs in the study by  $S$ . In the causal inference sub-models, all data and parameters are storm-specific and should be indexed by an  $s \in \{1, \dots, S\}$ . However, for clarity of presentation, we suppress these indices and introduce the causal inference concepts in the context of a single arbitrary TC. Let  $i = 1, \dots, N$  index the set of treated and control counties and  $t = 1, \dots, T$  index time

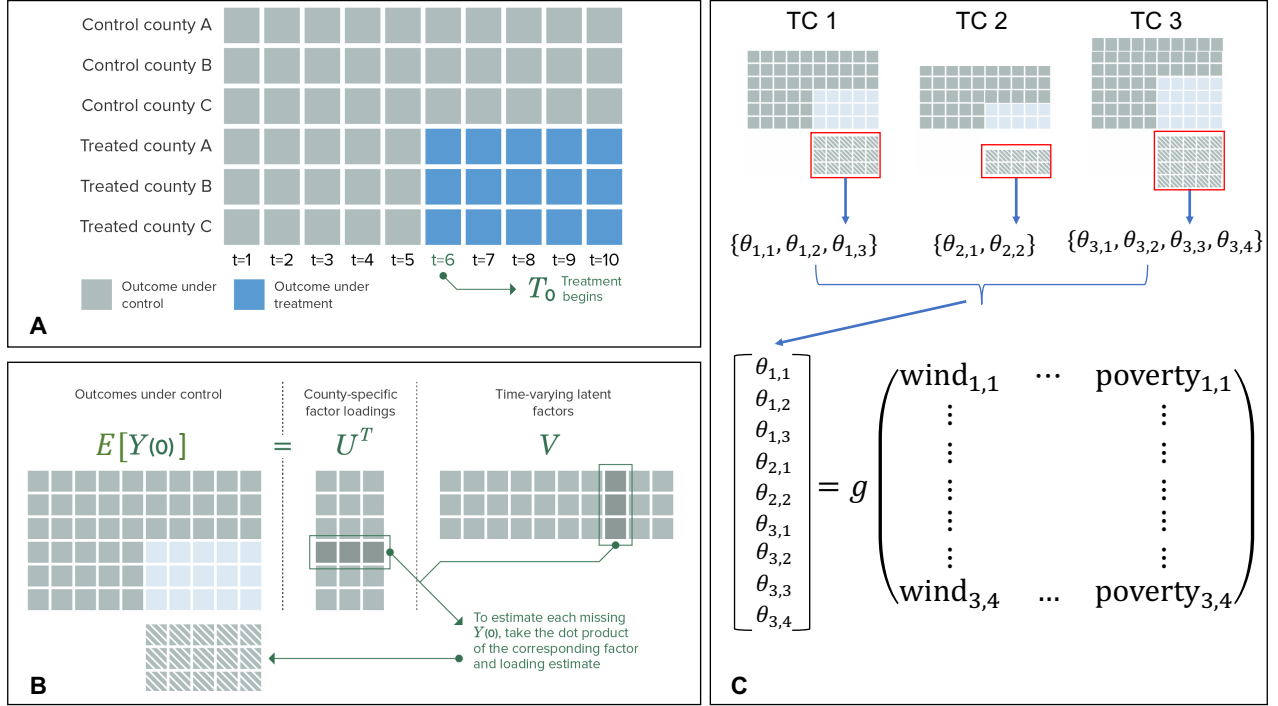


Figure 1: Example of panel data structure (A), illustration of matrix completion (B), and visual explanation of our integrated causal and predictive modeling approach (C).

windows, so that the panel data matrix (Figure 1A) has dimensions  $N \times T$ , with counties in the rows and times in the columns.

For a given TC, we assume that we have a set of “treated” and control counties, that all counties are untreated at  $t = 1$ , and that once treatment begins for treated counties they remain treated through  $t = T$ . We let  $W$  denote the set of indices of treated counties. Let  $D_{it}$  be a binary indicator of treatment of county  $i$  by the TC at time  $t$ . Let  $T_0$  denote the common time period when treatment is initiated in treated counties, such that all counties are untreated prior to  $T_0$ , and treatment occurs for treated counties at times  $T_0$  through  $T$  (see Figure 1A). While staggered treatment initiation times can be accommodated in this framework, we focus on a common treatment initiation time for clarity. Thus,  $D_{it} = 1$  if  $\{(i, t) : i \in W, t \geq T_0\}$ ,  $D_{it} = 0$  otherwise. Collectively, the set of all  $t \in [T_0, T]$  is referred to as the treatment period.

$Y_{it}$  is the observed number of health events for county  $i$  at time  $t$ , and the panel data matrix of the outcomes is denoted  $\mathbf{Y}$ . We formalize our causal inference approach using Rubin’s potential outcomes framework (Rubin, 1974), invoking assumptions given in Section S.3. In short, in treated counties during treatment, we observe the outcome that occurs under treatment and we wish to compare it to an estimate of the “counterfactual” outcome that would have occurred in the absence of treatment. Formally, let  $Y_{it}(0)$  be the potential outcome in county  $i$  at time  $t$  under control. For control counties at all times and for treated counties prior to the treatment period,  $Y_{it}(0) = Y_{it}$ . For treated counties during the treatment period, we instead observe the potential outcome under treatment,  $Y_{it}(1) = Y_{it}$ . The aim of the causal inference sub-model for each TC is to estimate the individual excess events (IEE), defined as  $\theta_i = \sum_{t \geq T_0} [Y_{it}(1) - Y_{it}(0)]$  for  $i \in W$ . Here the word individual refers to individual units of analysis, in our case counties. Because  $Y_{it}(1) = Y_{it}$  for  $\{(i, t) : i \in W, t \geq T_0\}$ , our aim is to estimate the counterfactual outcome,  $Y_{it}(0)$ .

Both spatial and temporal confounding are possible in studies of the health impacts of TCs. For example, coastal TC-prone counties may have wealthier populations and wealth is associated with health. Alternatively, TCs may be more likely to occur under certain climate conditions which may independently affect health outcomes. With most observational study designs, causal inference analyses rely on the assumption

of ignorable treatment assignment conditional on observed confounders (no unmeasured confounding). To flexibly address potentially unmeasured confounding, we conceptualize each TC as a quasi-experiment, i.e., a study design with nonrandomized treatment assignment but with pre- and post-treatment data available. In environmental health studies, quasi-experimental designs are the gold standard for assessing causality because certain types of unmeasured confounders can be controlled for by design (Dominici and Zigler, 2017).

Classic methods such as difference-in-differences allow for control for time-invariant unmeasured confounders. Recent machine learning approaches such as matrix completion (Athey et al., 2018) go further by allowing control for certain types of time-varying unmeasured confounders. This ability to adjust for time-varying unmeasured confounding is particularly critical in our TC application. Many potential confounders of TC health effects demonstrate complex seasonal patterns, e.g., employment (Krane and Wascher, 1999), use of homeless shelters (Colburn, 2017), and infectious disease proliferation, but measurements of these variables are unavailable at the space-time resolution needed.

To estimate the health impacts of a TC in each treated county, we propose an adaptation of the matrix completion (MC) approach for conducting causal inference on natural experiments using panel data (Athey et al., 2018; Tanaka, 2019; Pang et al., 2020). MC is a machine learning technique for imputing missing values in a matrix, learning from patterns in observed entries in both the rows and columns. In our setting, the matrix with missing entries is the matrix of  $Y_{it}(0)$  values, denoted by  $\mathbf{Y}(0)$ .  $\mathbf{Y}(0)$  is structured just like the panel data matrix, with missing entries in positions corresponding to the treated counties during the treatment period (Figure 1A, blue elements missing). MC learns from space-time trends in the non-missing data, i.e., the outcomes for (1) control counties at all time periods and (2) treated counties prior to treatment, to impute the missing  $Y_{it}(0)$ . In this approach, the observed  $Y_{it}(1)$  are treated as fixed and known and are entirely omitted from the MC model. In settings with normally distributed data, MC can be framed as a factorization of  $\mathbf{Y}(0)$  (or of its expectation), as illustrated in Figure 1B.

Because our outcomes are counts, we generalize the MC approach for causal inference to allow for count data likelihoods. MC models for count data were developed in other contexts (Gopalan et al., 2014), but do not follow epidemiologic conventions for modeling count data. We instead propose the following MC model for count data using a log link:

$$\log(E[Y_{it}(0)]) = \alpha + \gamma_i + \psi_t + \mathbf{U}_i^T \mathbf{V}_t + \log(p_{it}) \quad (1)$$

$\alpha$  is a global intercept,  $\gamma_i$  are county-specific deviations from the global intercept, and  $\psi_t$  are time-specific deviations.  $\mathbf{V}_t$  is a  $K$ -length ( $K \ll \min(N, T)$ , unknown) vector of unobserved factors influencing the  $Y_{it}(0)$  that vary over time but are common to all counties and  $\mathbf{U}_i$  is a  $K$ -length vector of the unobserved county-specific effects of the  $\mathbf{V}_t$  on  $Y_{it}(0)$ . Together, the  $\mathbf{V}_t$  and  $\mathbf{U}_i$  provide a low-dimensional representation of the space-time trends in the  $Y_{it}(0)$  (see Figure 1B for an illustration in the case of normally-distributed outcomes).  $p_{it}$  is a scalar population size offset, to allow for rate outcomes. We pre-specify  $K$  based on exploratory principal component analyses and fit the MC models using a negative binomial likelihood and uninformative prior distributions, collecting MCMC samples using the rstan (Stan Development Team, 2020) software package. Explicit modeling details are given in Section S.2. For a treated county  $i$  at post-treatment time  $t$ , we use the above model to collect  $M$  MCMC samples from the posterior predictive distributions of the missing counterfactuals, denoted  $Y_{it}^{(m)}(0)$  for  $m = \{1, \dots, M\}$ , and use those to construct  $M$  posterior samples of the IEE, as  $\theta_i^{(m)} = \sum_{t \geq T_0} \{Y_{it} - Y_{it}^{(m)}(0)\}$  for  $i \in W$ .

The formal causal identifying assumptions for this model, originally specified in (Pang et al., 2020) are provided in Section S.3. Under these assumptions, the  $\mathbf{U}_i^T \mathbf{V}_t$  should capture all space-time trends in the  $Y_{it}(0)$ , including trends induced by time-varying confounders. Thus the resulting IEE can be identified, assuming trends in confounders do not change differentially in treated units (relative to controls) post-treatment.

In practice, both the excess number of events and the excess rate of events (per unit population) are of interest for understanding the epidemiology of extreme weather events. Thus we define the individual

excess rate as  $\theta_i^* = 100000 \times (\theta_i/p_{iT})$ . We also define TC-specific excess events as the cumulative excess events across all counties impacted by a TC, and TC-specific excess rate as the excess rate across all impacted counties. To compare with existing literature and evaluate overall health burdens, we also wish to summarize the estimated health effects across our entire study. To this end, we define the total excess events (TEE) for the full study to be the cumulative TC-attributable excess events summed over all TCs and counties, and the average excess rate (AER) to be the average of the excess rates across all county-level TC exposures in the study. Formal definitions of each estimand are given in Table S.3. Posterior samples of these quantities can be constructed through simple transformations of the  $\theta_i^{(m)}$ .

### 2.2.2 Bayesian modularization

In a classic Bayesian framework, a full likelihood is specified for the data, and the model components are fit jointly, permitting unrestricted information flow. However, in many real-world contexts, there is a need to propagate uncertainty between model components without allowing information to flow bi-directionally between all model components. This may be due to philosophical considerations, as in the case of Bayesian propensity score methods (McCandless et al., 2010; Zigler et al., 2013), or practical considerations, as complex models fit jointly may suffer from poor mixing or require prohibitive computation times. These concerns have given rise to a literature on Bayesian modularization, in which information flows between certain sub-models weakly or not at all (Liu et al., 2009; Lunn et al., 2009; Plummer, 2015; Jacob et al., 2017). This is often achieved by ignoring some components of the joint likelihood.

We modularize our models in a manner that prevents information flow between the causal inference sub-models for each TC (as described above), yet allows information to flow uni-directionally from the causal models into the predictive model. This permits uncertainty in the TC health effect estimates to be accounted for when fitting the predictive model, but does not allow the predictive model to inform the causal effect estimates. Explicit details are provided in Section S.4. This modularization approach is motivated by both philosophy and computational feasibility. Primarily, we wish to prevent information from the predictive model from influencing the causal models, which would obscure the identifying assumptions needed to obtain causal effect estimates. Because our causal modeling approach is computationally intensive and involves many unidentifiable parameters, the modularization approach is also more practical, as it improves mixing and reduces computation time by enabling parallel model-fitting across TCs.

### 2.2.3 Predictive sub-model

We develop a predictive model for each health outcome that captures the relationship between the county-specific TC health effects and the features of the TC and county (i.e., characterizing how such features modify TC health impacts). For clarity in this section, we re-introduce the storm-specific indices, but continue to focus on a single outcome-specific model. We let  $\theta_{si}^{*(m)}$  be the individual excess rate posterior sample  $\theta_i^{*(m)}$  for TC  $s$ , and  $W_s$  be the set of indices of treated counties  $W$  for TC  $s$ . Then, for a single fixed posterior draw  $m$ , we collect a posterior sample of the parameters  $\beta$  from the (outcome-specific) predictive model:

$$\{\theta_{si}^{*(m)} = g(\mathbf{X}_{si}; \beta) \mid s \in \{1, \dots, S\}, i \in W_s\}$$

where  $\mathbf{X}_{si}$  is a vector of predictors, i.e., modifiers, of the county-specific TC effects, and  $g()$  is an unspecified function parameterized by a vector of global parameters  $\beta$ . In practice,  $g()$  could take the form of any Bayesian predictive model. We recommend selecting  $g()$  based on cross-validation performance. We repeat this sampling with each  $\theta_{si}^{*(m)}$  to obtain posterior samples  $\{\beta^{(1)}, \dots, \beta^{(M)}\}$  (Figure 1C).

### 2.2.4 Prediction for future TCs

Using the posterior samples  $\beta^{(m)}$ , we can draw corresponding posterior predictive samples of the health effect,  $\theta_{new}^{*(m)}$ , for any set of predictor values  $\mathbf{X}_{new}$ . To use the model for county-level prediction of the health

impacts of a specific approaching TC,  $\mathbf{X}_{new}$  could be defined as the forecasted meteorological characteristics of the TC and socioeconomic and demographic characteristics of each county on its expected path. The predicted health impacts and uncertainties for each county can be used to identify counties at highest health risk. Alternatively, to create a long-term TC health risk profile for a county, many different  $\mathbf{X}_{new}$  vectors could be created using the meteorological characteristics of a collection of hypothetical, representative TC exposures, as well as the socioeconomic and demographic characteristics of the county. The resulting set of predictions can be summarized to give insight into future TC health risks the community may face, in both expected and extreme TC scenarios.

### 3 Results

#### 3.1 Causal analysis

53 TCs and 2,135 corresponding county-level TC exposures occurring during the period 1999-2015 are included in our analysis (see inclusion criteria in Section S.1.3). In Table S.4, we provide the name and year of each TC included in our study, the number of treated and control counties used in its causal model, and the rate of each health outcome among the treated and controls during the 140-day period surrounding the storm. Figure S.8 maps the number of TC exposures by county. Coastal counties in the Carolinas and the Gulf Coast region are repeatedly exposed, with some receiving as many as 15 TC exposures during our 17-year study period. For a discussion of the possible impacts of TC-related population displacement on our analyses, see Section S.5.

We apply the MC models for each TC and health outcome with  $K = 4$  factors.  $K = 4$  was chosen because exploratory principal component analyses revealed that 4 factors explained around 70% of the variance in the  $\mathbf{Y}(0)$  matrices (Section S.6). This selection allows for preservation of critical variance without overfitting. We run the causal models using two separate MCMC chains, collecting 1000 post-burn-in samples from each chain. Traceplots of the  $Y_{it}^{(m)}(0)$  indicated convergence.

##### 3.1.1 TC- and county-level estimated health effects

Recall that our analysis defines the treatment period as only the final two-week time window (beginning two days prior to the storm’s first approach and ending 11 days after). Thus, the IEE for county  $i$  exposed to TC  $s$ , can be expressed simply as  $\theta_{si} = Y_{iT}(1) - Y_{iT}(0)$ , i.e., the excess health events attributable to the TC at time  $T$ . For each of the four health outcomes, we have generated posterior samples of the IEE for each county impacted by each TC. We use these to construct posterior samples of the excess rates and the summary quantities described in Section 2.2.1. Hereafter, we refer to the posterior means for each parameter as the “estimates” from our models. Figure 2 shows the county-level excess rate estimates, grouped by TC, for all TCs that impacted  $> 25$  counties. Figure S.9 gives the TC-specific excess rate estimates. Figure 3 displays the TC-specific excess event estimates and 95% credible intervals, and the county-level excess event estimates (IEE) are shown in Figure S.10. These results illustrate the heterogeneity in TC health effects across counties and across storms.

We find that on average a county’s mortality rate increases slightly, though not significantly, during the 2-week treatment period, compared to the mortality rate expected in the absence of TC (AER: 2.58, 95% CI [-1.69, 6.56]; TEE: 1228.86, 95% CI [-608.20, 2731.07]). TC exposures cause larger and significant increases, on average, in respiratory hospitalizations (AER: 8.58 [4.34, 11.86]; TEE: 2926.18 [1808.97, 3940.02]) and COPD hospitalizations (AER: 4.57 [2.13, 6.79]; TEE: 1532.80 [969.95, 2106.10]). For each of these outcomes, we note that Hurricanes Katrina and Rita, which impacted largely overlapping sets of counties in the same year (2005), produced some of the largest adverse impacts (on both the excess event and the rate scale). We find that Hurricane Sandy caused huge increases in these outcomes specifically on the excess events scale, which is likely attributable to its impacts on the densely populated New York City area. Moreover, for each of these outcomes, Figures 2 and S.10 suggest that counties experiencing higher TC windspeeds may be at increased risk.

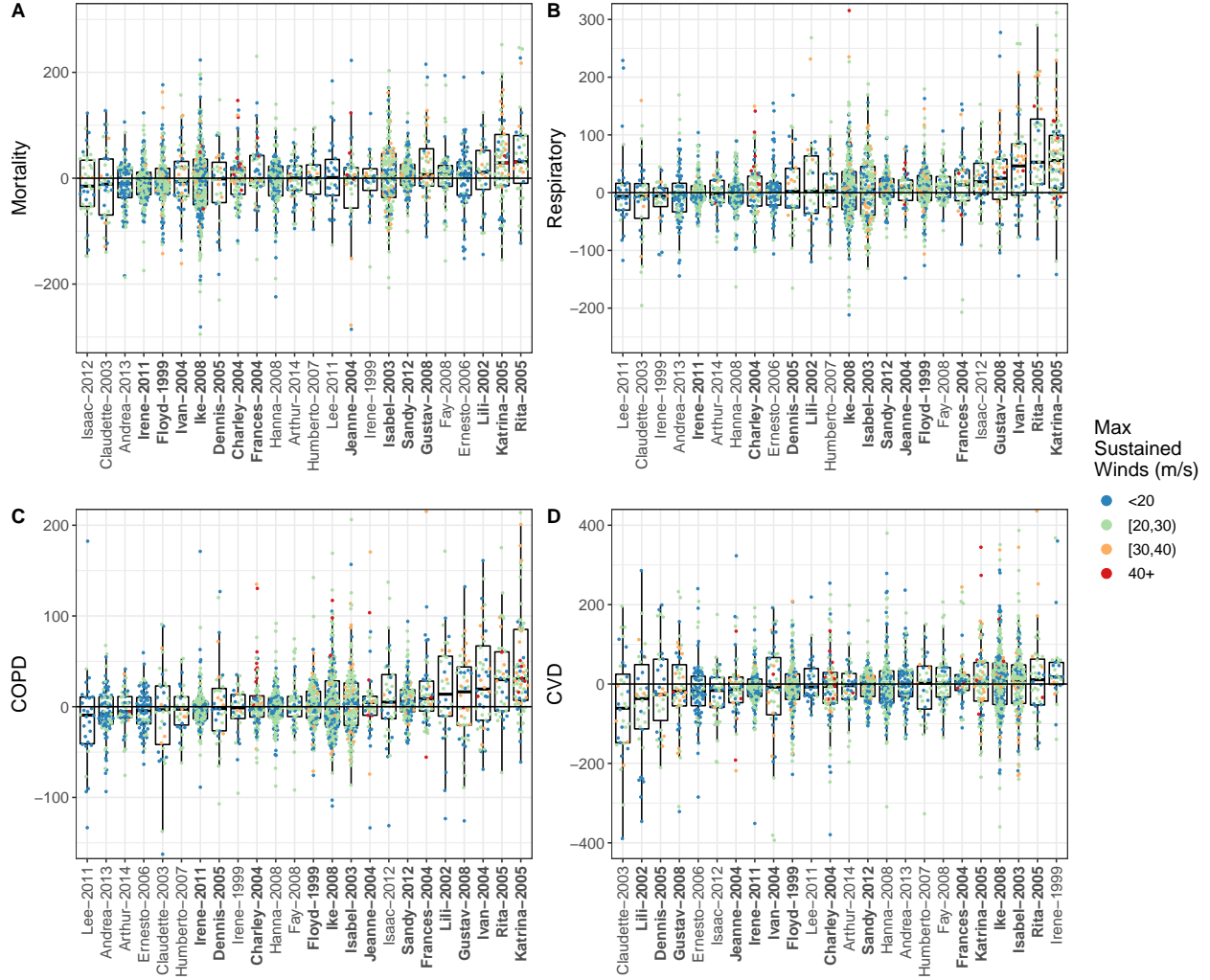


Figure 2: County-level excess rate estimates for mortality (A), respiratory hospitalizations (B), COPD hospitalizations (C), and CVD hospitalizations (D) for TCs that impacted  $> 25$  counties. The county excess rate is the estimated rate of excess events (per 100,000) in the county due to the TC. Distant outliers are cropped out for readability. Bolded TC labels indicate storm names that were subsequently retired—retirement occurs when a TC is so destructive that re-using the name is considered to be insensitive (National Hurricane Center, 2020).



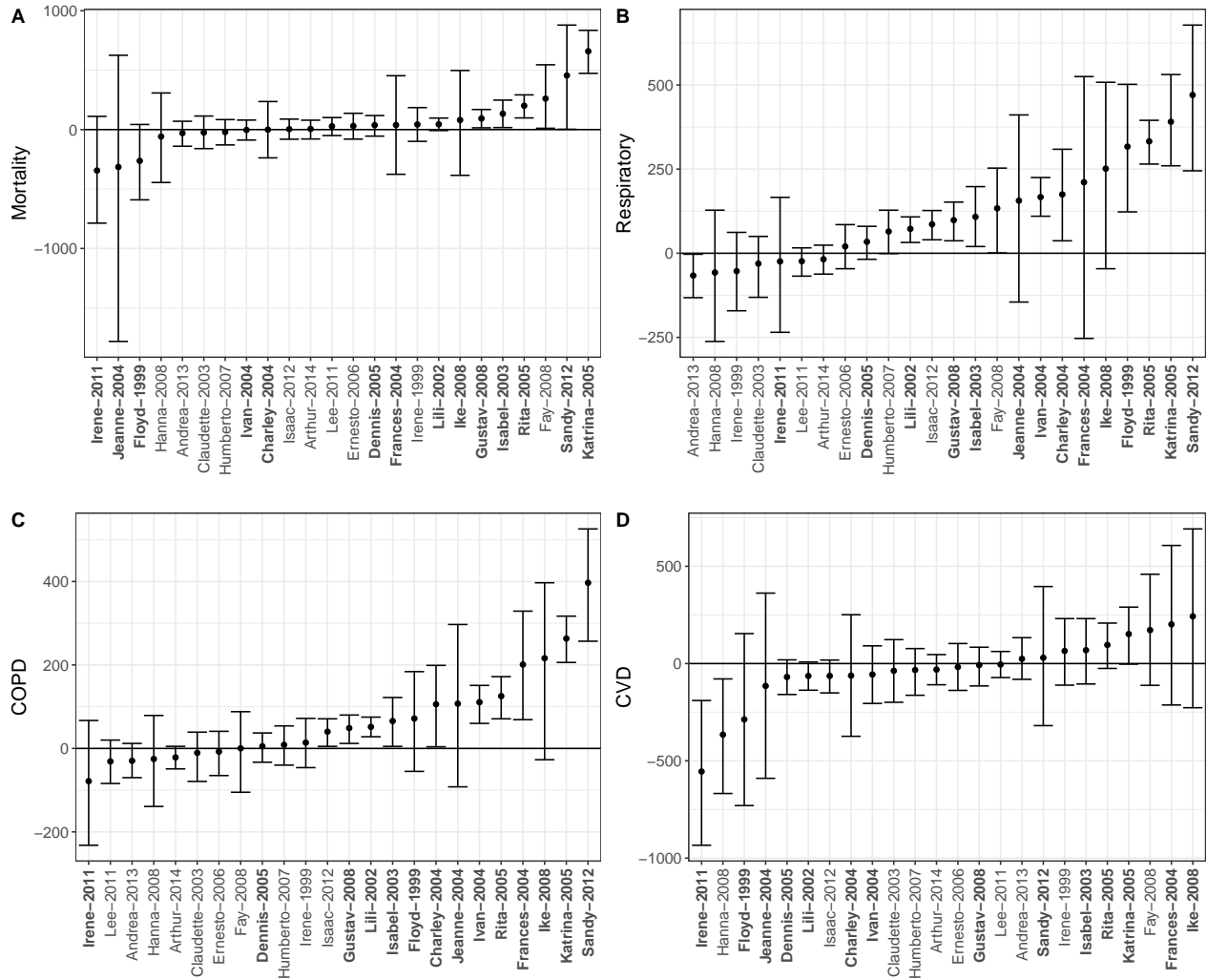


Figure 3: TC-specific excess events estimates and 95% predictive intervals for mortality (A), respiratory hospitalizations (B), COPD hospitalizations (C), and CVD hospitalizations (D) for TCs that impacted > 25 counties. The TC-specific excess events is the sum of excess event estimates across all counties impacted by the TC. Bolded TC labels indicate storm names that were subsequently retired—retirement occurs when a TC is so destructive that re-using the name is considered to be insensitive (National Hurricane Center, 2020).

For CVD, we find that hospitalization rates on average decrease during the 2-week period surrounding TC exposure (AER: -5.01 [-9.87, -0.30]; TEE: -977.99 [-2246.53, 222.10]). A previous study found decreases in CVD hospitalizations on the day of the storm but increases 2-3 days later (Yan et al., 2020). This finding is likely attributable in part to the fact that our hospitalization metric captures all inpatient hospitalizations, including planned procedures. The danger associated with venturing out during or immediately after a TC may motivate people to cancel planned procedures or treatment for chronic disease, so, while emergency CVD hospitalizations may have increased during the treatment period, the decrease in non-emergency CVD hospitalizations likely explains the overall reduction in CVD hospitalizations during the TC period.

### 3.2 Predictive analysis

The full set of candidate predictors is given in Section S.1.4. We conduct predictive model selection using cross-validation as described in Section S.7. The selected predictive model (common across health outcomes) is a Bayesian linear model with a spline on windspeed and year, with the remaining TC-related and socioeconomic/demographic predictors included as linear terms. For interpretability, we also provide results from a Bayesian linear regression model without the windspeed spline.

We fit the full modularized Bayesian models and obtain 1000 post-burn-in samples of the predictive model parameters. Tables S.5 and S.6 give the posterior means and 95% credible intervals for the predictive model coefficients. To illustrate the importance of propagating uncertainties from the causal to predictive modules of our model, we also overlay our predictive model estimates and 95% CIs with those obtained by implementing the causal and predictive models separately, i.e., without propagating uncertainty (Figure S.11).

In Figure 4, we show the windspeed splines and 95% credible intervals for each outcome. For each outcome, Table S.6 indicates that maximum sustained windspeed has the strongest association with health impacts, among the predictors considered. The splines illustrate that, as windspeeds increase beyond 30m/s, we observe a sharp increase in TC-attributable mortality and respiratory and COPD hospitalizations. While we generally find a similar trend for windspeed and CVD hospitalizations, the relationship is weaker and more variable.

We also find that TC-attributable respiratory hospitalizations are positively associated with the duration of sustained windspeeds above 20m/s (Table S.5). For respiratory and COPD hospitalizations, we observe a negative association with total number of TC exposures during the study period, a proxy for TC exposure propensity (Table S.5). This suggests that communities that are frequently hit may adapt in ways that decrease respiratory health impacts (e.g., bury power lines to decrease power outages, thereby decreasing risk for those dependent on electric-powered respiratory devices). Although few strong associations are detected for the county socioeconomic and demographic features, we find that predominately White communities tend to experience fewer TC-attributable COPD hospitalizations (Table S.5).

### 3.3 Sensitivity analyses

We conduct a range of sensitivity analyses for both the causal and predictive components of our model (Section S.8). For the causal models, we evaluate sensitivity to our definition of TC exposure and to specification of  $K$ . Because we have cumulative TC precipitation data only for years prior to 2012, we fit predictive models restricted to years 2011 and earlier and include a restricted cubic spline on cumulative precipitation as a predictor. In short, we find that our causal models are robust to these specifications and that precipitation is weakly, if at all, associated with the acute health impacts of TCs after adjusting for other factors.

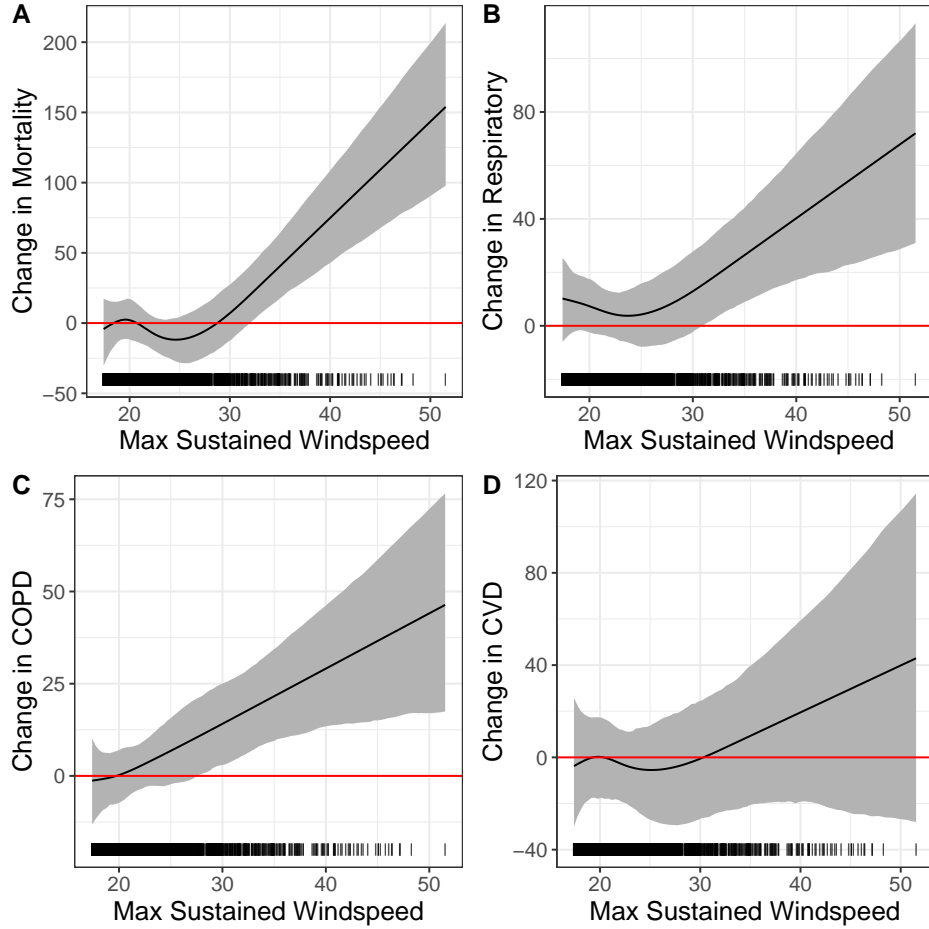


Figure 4: Relationship between maximum sustained windspeed and county-level excess rates per 100,000 of mortality (A), respiratory hospitalizations (B), COPD hospitalizations (C), and CVD hospitalizations (D).

## 4 Discussion

We have proposed and implemented an integrated causal and predictive modeling framework for systematically characterizing and predicting the health impacts of TCs in the US, in order to inform pre-storm strategic preparedness efforts. This work offers several contributions to the existing literature on TC epidemiology. First, we have used a standardized causal inference approach to estimate county-level TC-attributable excess mortality and excess respiratory, COPD, and CVD hospitalizations (with uncertainties) in the Medicare population for nearly all Atlantic-basin TCs 1999-2015. These excess event estimates provide a more complete picture of TC health burdens than post-storm surveillance efforts or single-storm studies. We have also found that, controlling for a number of demographic and meteorological predictors, the maximum sustained windspeed experienced by a county is a strong predictor of its TC-attributable increases in adverse health events, potentially providing insight into strategies to minimize future TC health burdens. Our predictive models may also be useful for identifying specific communities facing the highest risk from future TC, which is critical to avert the most severe health consequences. Finally, this modeling approach can be used analogously in the context of other extreme weather and climate events, including heat waves, droughts, floods, and wildfire smoke exposures.

More detailed data on the multi-dimensional TC exposures and pre-TC preparatory measures would improve the predictive ability of our models and provide greater insight into how to minimize TC health burdens. For instance, flooding is a common and often devastating TC-related exposure. While a county-level

binary indicator of TC flooding is available (Anderson et al., 2020), this is insufficient for understanding the impact of floods, which tend to be highly complex and localized. Additionally, mandatory pre-storm evacuation orders may be a critically influential factor in the health impacts of a TC; however, to our knowledge, evacuation data have never been systematically compiled on a multi-storm scale. To minimize the health threats presented by climate and weather disasters, we must continue to collect, compile, and analyze more and higher quality data on these events.

## **5 Acknowledgements**

The authors gratefully acknowledge funding from NIH grants R01HD092580, R01AG060232-01A1, R01ES028805, R01ES030616, P30ES009089, R00ES022631 and NSF grants NSF 1940141 and NSF 1331399.

## References

- Anderson, G. B., J. Ferreri, M. Al-Hamdan, W. Crosson, A. Schumacher, S. Guikema, S. Quiring, D. Edelbuettel, M. Yan, and R. D. Peng (2020). Assessing United States county-level exposure for research on tropical cyclones and human health. *In press, Environmental Health Perspectives*.
- Athey, S., M. Bayati, N. Doudchenko, G. Imbens, and K. Khosravi (2018). Matrix completion methods for causal panel data models. Technical report, National Bureau of Economic Research.
- BBC (2018). Puerto Rico increases Hurricane Maria death toll to 2,975. *BBC*.
- Brunkard, J., G. Namulanda, and R. Ratard (2008). Hurricane Katrina deaths, Louisiana, 2005. *Disaster Medicine and Public Health Preparedness* 2(4), 215–223.
- Centers for Disease Control and Prevention (2004). Preliminary medical examiner reports of mortality associated with Hurricane Charley—Florida, 2004. *Morbidity and Mortality Weekly Report* 53(36), 835.
- Centers for Disease Control and Prevention (2005). Surveillance for illness and injury after Hurricane Katrina—New Orleans, Louisiana, September 8–25, 2005. *MMWR: Morbidity and Mortality Weekly Report* 54(40), 1018–1021.
- Centers for Disease Control and Prevention (2013). Deaths associated with Hurricane Sandy—October–November 2012. *MMWR. Morbidity and Mortality Weekly Report* 62(20), 393.
- Chen, W.-d., C. Bin, C. Fang, Q. Jian, and D. Huang (2018). Impacts of Typhoon Meranti on distribution circuits of Xiamen. In *Proceedings of the 2018 4th International Conference on Green Materials and Environmental Engineering*.
- Colburn, G. (2017). Seasonal variation in family homeless shelter usage. *Housing Policy Debate* 27(1), 80–97.
- Dominici, F. and C. Zigler (2017). Best practices for gauging evidence of causality in air pollution epidemiology. *American Journal of Epidemiology* 186(12), 1303–1309.
- Dosa, D., K. Hyer, K. Thomas, S. Swaminathan, Z. Feng, L. Brown, and V. Mor (2012). To evacuate or shelter in place: implications of universal hurricane evacuation policies on nursing home residents. *Journal of the American Medical Directors Association* 13(2), 190–e1.
- Gong, Z., C. Chai, C. Tu, J. Lin, Y. Gao, and Y. Qiu (2007). Injuries after a typhoon in China. *New England Journal of Medicine* 356(2), 196–197.
- Gopalan, P. K., L. Charlin, and D. Blei (2014). Content-based recommendations with Poisson factorization. In *Advances in Neural Information Processing Systems*, pp. 3176–3184.
- Gotanda, H., J. Fogel, G. Husk, J. M. Levine, M. Peterson, K. Baumlin, and J. Habboushe (2015). Hurricane Sandy: impact on emergency department and hospital utilization by older adults in Lower Manhattan, New York (USA). *Prehospital and Disaster Medicine* 30(5), 496–502.
- Gray, B. H. and K. Hebert (2007). Hospitals in Hurricane Katrina: challenges facing custodial institutions in a disaster. *Journal of Health Care for the Poor and Underserved* 18(2), 283–298.
- Greenstein, J., J. Chacko, B. Ardolic, and N. Berwald (2016). Impact of hurricane sandy on the Staten Island University Hospital emergency department. *Prehospital and Disaster Medicine* 31(3), 335–339.
- Han, S.-R., S. D. Guikema, S. M. Quiring, K.-H. Lee, D. Rosowsky, and R. A. Davidson (2009). Estimating the spatial distribution of power outages during hurricanes in the Gulf Coast region. *Reliability Engineering & System Safety* 94(2), 199–210.

- Jacob, P. E., L. M. Murray, C. C. Holmes, and C. P. Robert (2017). Better together? Statistical learning in models made of modules. *arXiv preprint arXiv:1708.08719*.
- Keim, M. E. (2008). Building human resilience: the role of public health preparedness and response as an adaptation to climate change. *American Journal of Preventive Medicine* 35(5), 508–516.
- Kim, H., R. M. Schwartz, J. Hirsch, R. Silverman, B. Liu, and E. Taioli (2016). Effect of Hurricane Sandy on Long Island emergency departments visits. *Disaster Medicine and Public Health Preparedness* 10(3), 344–350.
- Kishore, N., D. Marquas, A. Mahmud, M. V. Kiang, I. Rodriguez, A. Fuller, P. Ebner, C. Sorensen, F. Racy, J. Lemery, L. Maas, J. Leaning, R. A. Irizarry, S. Balsari, and C. O. Buckee (2018). Mortality in Puerto Rico after Hurricane Maria. *New England Journal of Medicine*. PMID: 29809109.
- Klinger, C. and V. M. Owen Landeg (2014). Power outages, extreme events and health: a systematic review of the literature from 2011-2012. *PLoS Currents* 6.
- Krane, S. and W. Wascher (1999). The cyclical sensitivity of seasonality in us employment. *Journal of Monetary Economics* 44(3), 523–553.
- Lane, K., K. Charles-Guzman, K. Wheeler, Z. Abid, N. Graber, and T. Matte (2013). Health effects of coastal storms and flooding in urban areas: a review and vulnerability assessment. *Journal of Environmental and Public Health* 2013.
- Lenane, Z., E. Peacock, and M. Krousel-Wood (2017). Post-traumatic stress disorder associated with Hurricane Katrina predicts cardiovascular disease events among elderly adults. *Journal of Clinical and Translational Science* 1(S1), 24–24.
- Lew, E. O. and C. V. Wetli (1996). Mortality from Hurricane Andrew. *Journal of Forensic Science* 41(3), 449–452.
- Liu, F., M. Bayarri, J. Berger, et al. (2009). Modularization in Bayesian analysis, with emphasis on analysis of computer models. *Bayesian Analysis* 4(1), 119–150.
- Lunn, D., N. Best, D. Spiegelhalter, G. Graham, and B. Neuenschwander (2009). Combining MCMC with ‘sequential PKPD modelling. *Journal of Pharmacokinetics and Pharmacodynamics* 36(1), 19.
- Lutgendorf, S. K., M. H. Antoni, G. Ironson, M. A. Fletcher, F. Penedo, A. Baum, N. Schneiderman, and N. Klimas (1995). Physical symptoms of chronic fatigue syndrome are exacerbated by the stress of Hurricane Andrew. *Psychosomatic Medicine* 57(4), 310–323.
- McCandless, L. C., I. J. Douglas, S. J. Evans, and L. Smeeth (2010). Cutting feedback in bayesian regression adjustment for the propensity score. *The International Journal of Biostatistics* 6(2).
- McQuade, L., B. Merriman, M. Lyford, B. Nadler, S. Desai, R. Miller, and S. Mallette (2018). Emergency department and inpatient health care services utilization by the elderly population: Hurricane Sandy in the state of New Jersey. *Disaster Medicine and Public Health Preparedness* 12(6), 1–9.
- National Academies of Sciences, Engineering, and Medicine (2020). *A Framework for Assessing Mortality and Morbidity After Large-Scale Disasters*. Washington, DC: The National Academies Press.
- National Hurricane Center (2020 (accessed October 14, 2020)). *Tropical Cyclone Naming History and Retired Names*.
- National Oceanic and Atmospheric Administration (2020 (accessed September 2, 2020)). *Hurricane Costs*.

- Pang, X., L. Liu, and Y. Xu (2020). A Bayesian alternative to synthetic control for comparative case studies. *Available at SSRN*.
- Plummer, M. (2015). Cuts in Bayesian graphical models. *Statistics and Computing* 25(1), 37–43.
- Rappaport, E. N. (2014). Fatalities in the United States from Atlantic tropical cyclones: New data and interpretation. *Bulletin of the American Meteorological Society* 95(3), 341–346.
- Rappaport, E. N. and B. W. Blanchard (2016). Fatalities in the United States indirectly associated with Atlantic tropical cyclones. *Bulletin of the American Meteorological Society* 97(7), 1139–1148.
- Rivera, R. and W. Rolke (2018). Estimating the death toll of Hurricane Maria. *Significance* 15(1), 8–9.
- Rubin, D. B. (1974). Estimating causal effects of treatments in randomized and nonrandomized studies. *Journal of Educational Psychology* 66(5), 688.
- Sanchez, R. (2017). Workers laid off at now-closed Florida nursing home where 12 died. *CNN*.
- Santos-Burgoa, C., A. Goldman, E. Andrade, N. Barrett, U. Colon-Ramos, M. Edberg, A. Garcia-Meza, L. Goldman, A. Roess, J. Sandberg, et al. (2018). Ascertainment of the estimated excess mortality from Hurricane Maria in Puerto Rico. Technical report, Milken Institute of Public Health, The George Washington University.
- Santos-Lozada, A. R. and J. T. Howard (2018). Use of death counts from vital statistics to calculate excess deaths in Puerto Rico following Hurricane Maria. *Journal of the American Medical Association*.
- Sharma, A. J., E. C. Weiss, S. L. Young, K. Stephens, R. Ratard, S. Straif-Bourgeois, T. M. Sokol, P. Vranken, and C. H. Rubin (2008). Chronic disease and related conditions at emergency treatment facilities in the New Orleans area after Hurricane Katrina. *Disaster Medicine and Public Health Preparedness* 2(1), 27–32.
- Shultz, J. M. and S. Galea (2017). Preparing for the next Harvey, Irma, or Maria—addressing research gaps. *New England Journal of Medicine* 377(19), 1804–1806.
- Shultz, J. M., J. Russell, and Z. Espinel (2005). Epidemiology of tropical cyclones: the dynamics of disaster, disease, and development. *Epidemiologic Reviews* 27(1), 21–35.
- Stan Development Team (2020). RStan: the R interface to Stan. R package version 2.19.3.
- Swerdel, J. N., T. M. Janevic, N. M. Cosgrove, J. B. Kostis, et al. (2014). The effect of Hurricane Sandy on cardiovascular events in New Jersey. *Journal of the American Heart Association* 3(6), e001354.
- Tanaka, M. (2019). Bayesian matrix completion approach to causal inference with panel data. *arXiv preprint arXiv:1911.01287*.
- Thomalla, F. and H. Schmuck (2004). ‘We all knew that a cyclone was coming’: Disaster preparedness and the cyclone of 1999 in Orissa, India. *Disasters* 28(4), 373–387.
- Yan, M., A. Wilson, F. Dominici, Y. Wang, M. Al-Hamdan, W. Crosson, A. Schumacher, S. Guikema, S. Magzamen, J. L. Peel, R. D. Peng, and G. B. Anderson (2020). Tropical cyclone exposures and risks of emergency Medicare hospital admission for cardiorespiratory diseases in 175 urban United States counties, 1999–2010. *In press, Epidemiology*.
- Zigler, C. M., K. Watts, R. W. Yeh, Y. Wang, B. A. Coull, and F. Dominici (2013). Model feedback in Bayesian propensity score estimation. *Biometrics* 69(1), 263–273.

## S Supplementary Information: Integrated causal-predictive machine learning models for tropical cyclone epidemiology

### S.1 Data

#### S.1.1 Health outcomes

This study focuses on the following adverse health events: all-cause mortality, respiratory hospitalizations, chronic obstructive pulmonary disorder (COPD) hospitalizations, and cardiovascular disease (CVD) hospitalizations (ICD-9/10 codes given in Table S.1). These outcomes were selected based on evidence from previous TC research and a biologically plausible link to TC exposures (Yan et al., 2020). Each individual’s hospitalizations and death are assigned to their county of residence (not the county of hospitalization). We construct daily counts of CVD, respiratory, and COPD hospitalizations in the Medicare fee-for-service population for each county in the eastern US for the period 1999-2015. For this same set of counties, we also utilize daily county-level mortality counts in the entire Medicare population (not restricted to fee-for-service). When population denominators are used for the creation of incidence rates, the total Medicare population size is used for mortality outcomes, while the Medicare fee-for-service population size is used for hospitalization outcomes.

Table S.1: ICD-9/10 codes used to define each hospitalization type.

| Hospitalization Type                     | ICD-9   | ICD-10   |
|--|---|--|
| Cardiovascular Diseases                  | 390.xx–398.xx,<br>401.xx–405.xx,<br>410.xx–414.xx,<br>415.xx–417.xx,<br>420.xx–429.xx | I00–I52  |
| Respiratory Diseases                     | 464.xx–466.xx,<br>480.xx–487.xx,<br>490.xx–492.xx,<br>494.xx–496.xx                   | J04–J06, J20–<br>J21, J09–J18,<br>J40–J44, J47, J67                                    |
| Chronic Obstructive<br>Pulmonary Disease | 490.xx–492.xx,<br>494.xx–496.xx   | J40, J410, J411,<br>J449, J441, J440,<br>J418, J42, J439,<br>J479, J471, J670–<br>J679 |

#### S.1.2 TC exposures

To characterize county-level TC exposure, we leverage an open source data platform containing temporally-detailed track and feature data for each Atlantic-basin TC during the period 1999-2015 that came within 250km of at least one eastern US county. This data platform, which is made available through the `hurricaneexposedata` R package, has been fully described elsewhere (Anderson et al., 2017, 2019, 2020). Briefly, the TC tracks are obtained from the US National Hurricane Center’s “Best Tracks” dataset, which records the storm’s position every 6 hours, and the storm’s position is interpolated to 15-minute intervals. Wind fields are then modeled at 15-minute intervals, and the resulting values are used to estimate the storm’s maximum sustained windspeed at the population centroid of each US county (see Figure S.1). Cumulative precipitation amounts in each county associated with the TC are estimated by summing rainfall amounts from the North American Land Data Assimilation System Phase 2 (NLDAS-2) re-analysis dataset



(Rui and Mocko, 2014) over a 4-day window beginning two days prior to the storm’s closest approach to the county (these precipitation data are currently available only for years 1999-2011). The county-level wind and precipitation exposure metrics have undergone validation for use in epidemiologic studies (Anderson et al., 2020).

While the continuous windspeed and rainfall metrics are employed in the predictive component of the model, for the causal inference component we must define a binary metric of TC exposure, which we refer to as “treatment” for consistency with the causal inference literature. Counties exposed to the TC are referred to as treated counties and those not exposed as control counties. Because previous epidemiologic research has suggested that TC windspeed is the feature most associated with acute health impacts (Yan et al., 2020), we use a maximum sustained windspeed threshold to classify counties as treated or control. Moreover, because TC windfields are large and relatively homogeneous over small areas, their use to define TC exposure reduces within-county variation and the potential for exposure misclassification. We classify a county as treated for a given storm if it experienced sustained gale-force or higher sustained wind speeds ( $\geq 17.4$  meters/second); otherwise, the county is classified as a control (Yan et al., 2020). This threshold is consistent with the outer limit wind threshold used in the US National Hurricane Center’s wind radii product for characterizing tropical cyclone size.

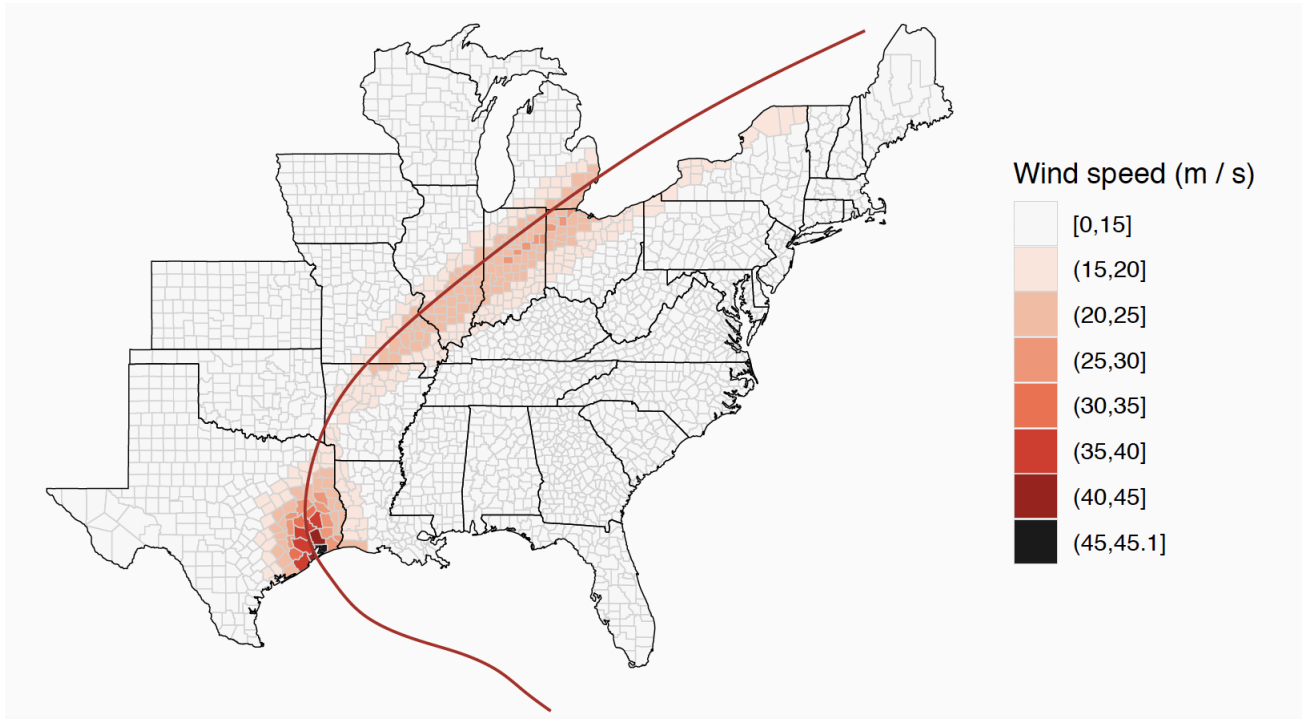


Figure S.1: Illustration of TC track and wind exposure measure for Hurricane Ike, 2008.

### S.1.3 Exposure and health data linkage

Our analytic approach requires defining a study period for each TC, composed of a substantial time span prior to the storm (used to establish baseline trends in health outcomes in treated and control counties) as well as the period during and immediately after the storm (to estimate acute storm effects). For each TC, we define its study period as beginning 129 days prior to the TC’s first US approach and ending 11 days after. The TC’s first approach is the earliest date that the TC makes its closest approach to an exposed US county/counties, which can be obtained from the `hurricaneexposedata` package (Anderson et al., 2020). In practice, the approximately 18 weeks of outcome data prior to the TC exposure for each county is aggregated into nine two-week counts of the outcome. Two-week cumulative counts are used because

narrower time intervals leads to small counts and instability in time series for many counties. We choose to employ nine of these two-week counts because (1) this provides enough time points to reveal relationships in baseline trends in the health outcomes in treated vs. control counties while (2) the time series covers a limited enough period that relationships between the time trends in treated and control counties would be expected to remain stable. The use of longer time series may introduce unnecessary noise into the models by capturing irrelevant long-term changes in relationships in baseline health across counties.

After designating each county in the study as treated or control for each TC as described above, we select a set of analytic treated and control counties for a given TC as follows. Any county (treated or control) is automatically excluded from the analytic set for a given TC if it has Medicare fee-for-service population size less than 100, or if it experiences 5 or fewer of any of the health events under study during the TC study period. Further, among the control counties, we select as analytic controls only those that fall within 150 miles of at least one treated county (distance computed between county centroids). Hereafter, when we reference the treated/control counties for a given TC, we are referring to the analytic treated/controls as defined here. We exclude TCs from the analysis if they have no valid treated counties, total sample size (treated + control counties) less than 20, or less than 5 control counties.

For each TC and each health outcome, we create a matrix of panel data, and these are central to the causal inference component of our model. The panel data matrix is composed of rows corresponding to each county in the analytic set for the given TC. Each row contains a time series of counts of the outcome in that county, for each two-week interval during the TC study period. This results in 10 two-week intervals, i.e., 10 columns in the panel data matrix. We then define each time period for each county as a control period or treatment period. For the control counties, all time periods represented in the panel data matrix are control periods. For treated counties, we consider the final two-week period, beginning 2 days before and ending 11 days after the TC’s first approach, to be the treatment period.

#### S.1.4 County and storm-specific features

Our predictive model will be used to capture the association between a TC’s health impacts and the TC’s meteorological features and the socioeconomic and demographic characteristics of the affected communities. To this end, for the predictive component of our model, we utilize the following TC features, which are described in more detail by Anderson et al. (2020), for each TC-county pair (abbreviated variable name in parentheses): modeled maximum sustained wind speed at the population centroid of the county during the TC (`vmax_sust`), duration of sustained wind speeds above 20 m/s at the population centroid of the county during the TC (`sust_dur`), year the TC occurred (`year`), and total number of TC exposures experienced by the county during 1999-2015 (`exposure`), which is a proxy for TC exposure propensity. For years 1999-2011, cumulative precipitation (`precip`) over a 4-day window, beginning two days prior to the TC’s closest approach, is also available from the `hurricaneexposedata` package. Because TC precipitation data are not available for our full study period, we use it only for sensitivity analyses for the predictive models.

We also consider the following spatial, demographic, and socioeconomic features of the county: percent of residents in poverty (`poverty`), percent of residents self-identifying as White (`white_pct`), percent of homes that are owner-occupied (`owner_occupied`), percent of residents age 65+ (`age_pct_65_plus`), population density (`population_density`), median house value (`median_house_value`), percent of residents without a high school degree (`no_grad`), a binary indicator of whether the county is located along the coastline (`cc1`), and the state the county is located in (`state`). These variables are extracted from US Census Bureau products. In particular we rely on the decennial census and American Community Survey (ACS). We align the demographic and socioeconomic features for each TC-county pair with the year of TC exposure. For years when census or ACS values are available, we use them directly, and in years not covered by the ACS or decennial census, we rely on interpolated values.

## S.2 Bayesian MC model fitting details

Numerous Bayesian approaches to MC model fitting have been proposed (Lim and Teh, 2007; Salakhutdinov and Mnih, 2008; Gopalan et al., 2014; Yang et al., 2018), and have been studied in the context of MC for causal inference (Tanaka, 2019; Pang et al., 2020). Without further restrictions on the MC model, the elements of  $\mathbf{U}$  and  $\mathbf{V}$  are not uniquely identified (only identified up to an orthogonal rotation). However, in a Bayesian framework, the presence of unidentifiable parameters in the model does not compromise the estimation of identifiable parameters. Here, our interest lies in estimating  $E[Y_{it}(0)]$  for missing entries, which is identifiable. Therefore, we allow  $\mathbf{U}$  and  $\mathbf{V}$  to remain unidentifiable and utilize instead the posterior distribution of  $E[Y_{it}(0)]$  and the posterior predictive distribution of  $Y_{it}(0)$  for inference.

Bayesian estimation proceeds by first specifying a data likelihood and prior distributions for the parameters. We specify the following likelihood:

$$P(Y(0)|\mathbf{U}, \mathbf{V}, \eta) = \prod_i \prod_t [f(Y_{it}(0)|\mathbf{U}_i, \mathbf{V}_t, \eta)]^{1-D_{it}}$$

where  $f$  is a negative binomial probability mass function with mean given by Equation 1, and a common scale parameter  $\eta$ . We fit the MC models using `rstan` (Stan Development Team, 2020), and to increase mixing and facilitate convergence we use the default flat prior distributions in Stan. Letting  $U_{ki}$  be the element in the  $k^{th}$  row and  $i^{th}$  column of  $\mathbf{U}$  and  $V_{kt}$  be the element in the  $k^{th}$  row and  $t^{th}$  column of  $\mathbf{V}$ , then prior distributions are specified as follows:

$$\begin{aligned} U_{ki} &\sim \text{Uniform}(-\infty, \infty) \\ V_{kt} &\sim \text{Uniform}(-\infty, \infty) \\ \eta &\sim \text{Uniform}(0, \infty) \end{aligned} \tag{2}$$

For each parameter, we sample from its distribution conditional on all of the other parameters in the same causal sub-model using MCMC sampling.

### S.3 Causal identifying assumptions

In the most general setting, the potential outcomes for our panel data would be defined as  $\mathbf{Y}(\mathbf{d})$ , a matrix containing all outcomes when treatment statuses for all units at all time points are given by the matrix  $\mathbf{d}$ . In this general case, each unit's potential outcomes depend on the treatment status of all units at all time points. In order to define the potential outcomes more concisely as we have in the paper, we invoke the classic Stable Unit Treatment Value Assumption used in causal inference (Rubin, 1980), which states that 1) there is only one version of treatment and that 2) one unit's outcome is unaffected by the treatment status of other units. If SUTVA is met, then we can define a unit's potential outcomes at time  $t$  as  $Y_{it}(\mathbf{d}_i)$ , where  $\mathbf{d}_i$  is a binary  $T$ -length vector of the treatment status of unit  $i$  at times  $1, \dots, T$ .

In order to define a unit's potential outcomes at time  $t$  as a function of only its treatment status at time  $t$ , as we have done in the main text, we are implicitly making the standard assumption that future treatment cannot impact past outcomes and making an additional assumption about the impact of treatment histories. That is, we assume that a unit's full historic treatment status vector is a deterministic function of the unit's time of initial treatment adoption, so a unit's potential outcomes can be expressed as functions of only the unit's time of initial treatment adoption, rather than functions of its full historic treatment status vector. The panel data construction described in the main text is designed to satisfy this assumption, by requiring that treated units initiate treatment at some time  $T_0 > 1$  and remain treated through time  $T$ . In general, we can allow for varying initiation times by unit, denoted by  $T_{0i}$ . In this setting, the treatment assignment vector  $\mathbf{d}_i$  is determined entirely by treatment initiation time  $T_{0i}$ , such that we can write the observed treatment vector as  $\mathbf{d}_i(T_{0i})$ . Under this assumption, we can write  $Y_{it}(\mathbf{d}_i = \mathbf{0}) = Y_{it}(0)$ , since treatment history is fully determined for a unit that has not yet initiated treatment. For treated units, because  $Y_{it}(\mathbf{d}_i(T_{0i}))$  is observed when  $t \geq T_{0i}$ , it can be treated as a known quantity and simplified to  $Y_{it}(1)$ . Then for  $i \in W$ ,  $t \geq T_{0i}$  we can define the IEE as  $\theta_i = \sum_{t \geq T_0} [Y_{it}(1) - Y_{it}(0)]$ .

We posit 4 additional assumptions that are needed to identify the causal effects of a TC using the proposed matrix completion approach.

*Assumption 1: Causal consistency.* This assumption states that the observed outcome is equal to the potential outcome under the observed treatment level, i.e.,

$$Y_{it}(d) = Y_{it} \text{ if } D_{it} = d$$

*Assumption 2: Latent ignorability.* Let  $\mathbf{Y}_i(\mathbf{0})$  be the vector of outcomes under control for unit  $i$  and  $\mathbf{Y}_i(\mathbf{0})^{obs}$  be the observed elements of  $\mathbf{Y}_i(\mathbf{0})$ . This assumption states that conditional on observed covariates used in the causal model,  $\mathbf{Z}_i$  (if any are used), the latent variables,  $\mathbf{U}_i' \mathbf{V}$ , and the observed outcomes under control,  $\mathbf{Y}_i(\mathbf{0})^{obs}$ , the treatment assignment is independent of the potential outcomes under control. This assumption is analogous to, but weaker than, the classic ignorability assumption required for causal inference, because it allows for unmeasured confounding to be captured either by observed variables, or by the time-varying latent variable. Formally, this assumption is written as

$$T_{0i} \perp \mathbf{Y}_i(\mathbf{0}) \mid \mathbf{Y}_i(\mathbf{0})^{obs}, \mathbf{Z}_i, \mathbf{U}_i^T \mathbf{V}$$

*Assumption 3: Approximation of unobservables.* This assumption states that the matrix of unobserved features impacting the outcomes over time can be approximated through a low-rank matrix factorization. Equivalently, this requires that the unobserved time-varying confounders can be captured by a small number of latent factors,  $K$ , defined by the matrix factorization. This assumption is analogous to the assumption of correct model specification in standard regression models, but adapted to the context of latent variable models. Formally, this assumption requires that, for each unit, there is a latent (possibly time-varying) confounder of the treatment effect,  $\mathbf{W}_i$ , that can be approximated by a low-rank matrix

factorization  $\mathbf{W}_i = \mathbf{U}_i^T \mathbf{V}$ .

*Assumption 4: Conditional exchangeability.* Conditional on any observed covariates  $\mathbf{Z}$ , and latent variable  $\mathbf{W}$ , elements of  $\mathbf{Y}(\mathbf{0})$  are exchangeable. This assumption is needed in order to define the posterior predictive distribution used to estimate the missing values in  $\mathbf{Y}(\mathbf{0})$ .

Under these assumptions, Pang et al. (2020) show that the causal effects are identified by Bayesian matrix completion models.

## S.4 Bayesian modularization

Our modularized model can also be viewed as a complex Bayesian multiple imputation procedure. Causal inference in the potential outcomes framework is often treated as a missing data problem, i.e., the counterfactual outcomes are considered missing data that needs to be imputed. In our case, the TC-specific causal inference models are used to impute counterfactual outcomes, and the resulting treatment effects from all the TCs are passed into the predictive model. Although the causal and predictive models suggest incompatible distributions for the missing counterfactual outcomes, the use of incompatible imputation and analysis models has been well-studied. This approach, often referred to as a fully conditional model specification, incompatible Markov Chain Monte Carlo (MCMC), or multiple imputation with incongenial sources of input, has been shown to often perform better than fully Bayesian data augmentation with complex models (Meng, 1994; Rubin, 2003; Schafer, 2003; Van Buuren et al., 2006; Van Buuren, 2007; Kuo and Wang, 2018).

We introduce our modularization approach using this missing data perspective. Our goal is to illustrate the principles used to modularize the model by providing general forms of the modularized full conditional distributions of all parameters. For a given TC  $s$ , denote by  $Y_s(0)$  the full set of potential outcomes under control, composed of both the observed values  $Y_s^{obs}(0)$  and the missing values  $Y_s^{mis}(0)$ . The causal component of the model aims to estimate the  $Y_s^{mis}(0)$ . Denote the TC-specific causal parameters by  $\phi_s$  and denote the treatment indicators for each unit/time collectively as  $D_s$  (note that from the missing data perspective, the treatment indicators can be viewed as missingness indicators). We assume throughout this section that  $Y_s(1)$ , the (observed) potential outcomes under treatment for the treated units at post-treatment times, are fixed and known quantities. Then the IEEs,  $\theta_s$ , are assumed to be a deterministic function of the  $Y_s^{mis}(0)$ . In the predictive component of the model, let  $X$  denote the predictors and  $\beta$  denote the predictive model parameters. (We again focus on a single outcome-specific model.)

Then the posterior distribution of the parameters and missing data can be expressed as

$$P\left(\left\{Y_s^{mis}(0)\right\}_{s=1}^S, \left\{\phi_s\right\}_{s=1}^S, \beta \mid \left\{Y_s^{obs}(0)\right\}_{s=1}^S, \left\{D_s\right\}_{s=1}^S, X\right)$$

Traditional Bayesian MCMC sampling algorithms successively sample from the full conditional posterior distribution of each of the unknown parameters. For the missing data, we obtain the following full conditional distribution

$$\begin{aligned} P\left(\left\{Y_s^{mis}(0)\right\}_{s=1}^S \mid \left\{Y_s^{obs}(0)\right\}_{s=1}^S, \left\{D_s\right\}_{s=1}^S, X, \left\{\phi_s\right\}_{s=1}^S, \beta\right) &\propto P\left(\left\{Y_s^{obs}(0)\right\}_{s=1}^S, \left\{Y_s^{mis}(0)\right\}_{s=1}^S, \left\{D_s\right\}_{s=1}^S, X \mid \left\{\phi_s\right\}_{s=1}^S, \beta\right) \\ &= P\left(\left\{D_s\right\}_{s=1}^S \mid \left\{Y_s^{obs}(0)\right\}_{s=1}^S, \left\{Y_s^{mis}(0)\right\}_{s=1}^S, X, \left\{\phi_s\right\}_{s=1}^S, \beta\right) \times \\ &\quad P\left(\left\{Y_s^{obs}(0)\right\}_{s=1}^S \mid \left\{Y_s^{mis}(0)\right\}_{s=1}^S, X, \left\{\phi_s\right\}_{s=1}^S, \beta\right) \times \\ &\quad P\left(\left\{Y_s^{mis}(0)\right\}_{s=1}^S \mid X, \left\{\phi_s\right\}_{s=1}^S, \beta\right) \times \\ &\quad P\left(X \mid \left\{\phi_s\right\}_{s=1}^S, \beta\right) \end{aligned}$$

Then if we assume that

$$\left\{D_s, Y_s^{miss}(0), Y_s^{obs}(0)\right\} \perp\!\!\!\perp \left\{D_{s'}, Y_{s'}^{miss}(0), Y_{s'}^{obs}(0)\right\}_{s' \neq s} \mid \phi_s$$

we obtain

$$\prod_{s=1}^S P\left(D_s \mid Y_s^{obs}(0), Y_s^{mis}(0), X, \phi_s, \beta\right) P\left(Y_s^{obs}(0) \mid Y_s^{mis}(0), X, \phi_s, \beta\right) P\left(Y_s^{mis}(0) \mid X, \phi_s, \beta\right) P\left(X \mid \left\{\phi_s\right\}_{s=1}^S, \beta\right)$$

Then assuming the causal identifying assumptions hold, we have unconfoundedness conditional on the causal model parameters, so that  $P\left(D_s \mid Y_s^{obs}(0), Y_s^{mis}(0), X, \phi_s, \beta\right) = P\left(D_s \mid Y_s^{obs}(0), X, \phi_s, \beta\right)$ , which does not depend on  $Y_s^{mis}(0)$  and thus drops out.  $P\left(X \mid \left\{\phi_s\right\}_{s=1}^S, \beta\right)$  also does not depend on  $Y_s^{mis}(0)$

and drops out. This leaves us with the following full conditional distribution

$$P\left(\left\{Y_s^{mis}(0)\right\}_{s=1}^S \mid \left\{Y_s^{obs}(0)\right\}_{s=1}^S, \{D_s\}_{s=1}^S, X, \{\phi_s\}_{s=1}^S, \beta\right) \propto \prod_{s=1}^S P\left(Y_s^{obs}(0) \mid X, \phi_s, \beta\right) P\left(Y_s^{mis}(0) \mid X, \phi_s, \beta\right)$$

This distribution factorizes so that the  $Y_s^{mis}(0)$  can be sampled separately for each TC. Moreover, conditional on the causal model parameters,  $Y_s^{obs}(0)$  and  $Y_s^{mis}(0)$  do not depend on  $X$  or  $\beta$  so that

$$P\left(\left\{Y_s^{mis}(0)\right\}_{s=1}^S \mid \left\{Y_s^{obs}(0)\right\}_{s=1}^S, \{D_s\}_{s=1}^S, X, \{\phi_s\}_{s=1}^S, \beta\right) \propto \prod_{s=1}^S P\left(Y_s^{obs}(0) \mid Y_s^{mis}(0), \phi_s\right) P\left(Y_s^{mis}(0) \mid \phi_s\right)$$

and sampling of  $Y_s^{mis}(0)$  can be conducted separately for each TC and without integrating feedback from the predictive component of the model. The derivation of the full conditional distribution for the  $\{\phi_s\}_{s=1}^S$  proceeds similarly, i.e.,

$$\begin{aligned} P\left(\{\phi_s\}_{s=1}^S \mid \left\{Y_s^{obs}(0)\right\}_{s=1}^S, \left\{Y_s^{mis}(0)\right\}_{s=1}^S, \{D_s\}_{s=1}^S, X, \beta\right) &= P\left(\left\{Y_s^{obs}(0)\right\}_{s=1}^S, \left\{Y_s^{mis}(0)\right\}_{s=1}^S, \{D_s\}_{s=1}^S, X, \{\phi_s\}_{s=1}^S, \beta\right) \\ &= P\left(\left\{Y_s^{obs}(0)\right\}_{s=1}^S, \left\{Y_s^{mis}(0)\right\}_{s=1}^S, \{D_s\}_{s=1}^S \mid X, \{\phi_s\}_{s=1}^S, \beta\right) \times \\ &\quad P\left(X \mid \{\phi_s\}_{s=1}^S, \beta\right) \times P\left(\beta \mid \{\phi_s\}_{s=1}^S\right) \times P(\{\phi_s\}_{s=1}^S) \\ &\propto P\left(X \mid \{\phi_s\}_{s=1}^S, \beta\right) \times P\left(\beta \mid \{\phi_s\}_{s=1}^S\right) \\ &\quad \prod_{s=1}^S P\left(Y_s^{obs}(0), Y_s^{mis}(0) \mid \phi_s, \beta\right) P(\phi_s) \end{aligned}$$

Following conventions in the modularization literature, the  $P\left(X \mid \{\phi_s\}_{s=1}^S, \beta\right) P\left(\beta \mid \{\phi_s\}_{s=1}^S\right)$  term can be dropped from this full conditional to prevent feedback, and sampling of the  $\phi_s$  can proceed separately by TC and disjoint from the predictive model.

Finally, the full conditional for  $\beta$  can be expressed as

$$\begin{aligned} P\left(\beta \mid \left\{Y_s^{obs}(0)\right\}_{s=1}^S, \left\{Y_s^{mis}(0)\right\}_{s=1}^S, \{D_s\}_{s=1}^S, X, \{\phi_s\}_{s=1}^S\right) &\propto P\left(\left\{Y_s^{obs}(0)\right\}_{s=1}^S, \left\{Y_s^{mis}(0)\right\}_{s=1}^S, \{D_s\}_{s=1}^S, X, \{\phi_s\}_{s=1}^S, \beta\right) \\ &= P\left(\left\{Y_s^{obs}(0)\right\}_{s=1}^S, \left\{Y_s^{mis}(0)\right\}_{s=1}^S, \{D_s\}_{s=1}^S \mid X, \{\phi_s\}_{s=1}^S, \beta\right) \times \\ &\quad P\left(X \mid \{\phi_s\}_{s=1}^S, \beta\right) \times P\left(\beta \mid \{\phi_s\}_{s=1}^S\right) \times P(\{\phi_s\}_{s=1}^S) \\ &\propto P\left(X \mid \{\phi_s\}_{s=1}^S, \beta\right) P\left(\beta \mid \{\phi_s\}_{s=1}^S\right) \end{aligned}$$

Thus  $\beta$  is sampled conditional on the causal model parameters, allowing information from the causal models to flow into the predictive model. This is the rationale that guides our modularization approach.

Our full modularized model can be represented as the directed graphical model in Figure S.2. The one-way flow of information from the causal sub-models to the predictive model is depicted by the cuts in the arrows in Figure S.2. The MCMC sampling algorithm proceeds as follows. First, for each TC,  $s \in \{1, \dots, S\}$ , we fit our causal sub-model, drawing a posterior sample of the IEE for each affected county denoted by  $\theta_{is}^{(m)}$  for county  $i \in W_s$  and posterior sample  $m$  ( $m = 1, \dots, M$ ). We then update the predictive model parameters conditional on the IEE draw. We draw a posterior sample,  $\beta^{(m)}$ , of the parameters from this predictive model and iterate this procedure until convergence of all parameters in all models.

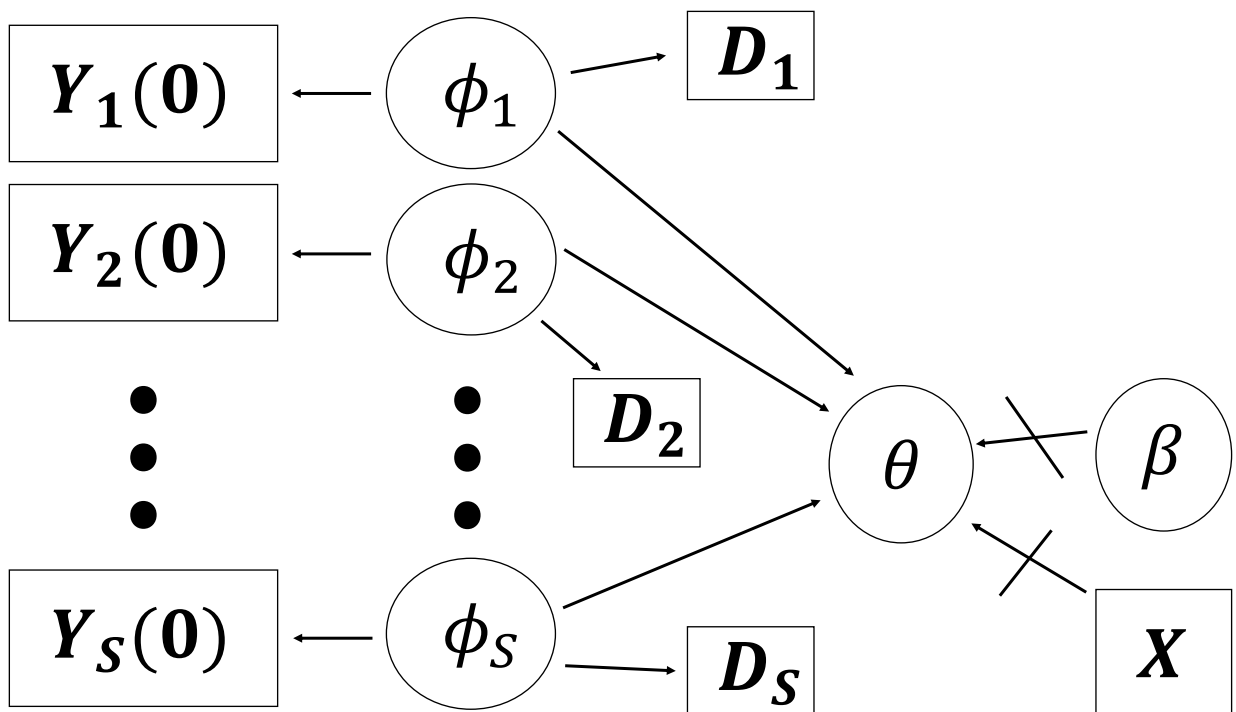


Figure S.2: DAG for Bayesian modularization



## S.5 Population displacement

The zipcode/county of residence recorded in Medicare claims data for each recipient is updated yearly and represents their place of residence at either the end of the specified year or early the following year (timing changes slightly year-to-year). This implies that, if a person moves from county A to county B during a given year, all their hospitalizations for that year will be assigned to county B. Because the Atlantic hurricane season occurs primarily in the latter half of the year (June-November), use of the county of residence at year’s end for exposure classification and population denominator construction is generally appropriate.

Yet, for a few severe storms that resulted in substantial long-term population displacement, such as Hurricane Katrina (Deryugina and Molitor, 2018), some degree of exposure misclassification is likely. However, we would expect that the impact of any such exposure misclassification would be to bias IEEs towards the null. Consider a scenario in which county A is exposed to a TC and county B is a control for that TC. Then, if a person living in county A at the time of exposure is hospitalized due to the TC, but is displaced to county B before the end of the year, their TC-attributable hospitalizations will be assigned to control county B. The resulting increase in adverse event rates in control counties should lead to an upward bias in the estimated  $Y_{it}(0)$ ,  $t \geq T_0$  and a corresponding downward bias in the IEE for the exposed counties. In spite of this potential for underestimated IEEs, we estimate large adverse health impacts for Hurricane Katrina. For most other TCs assessed by our study, we would expect that TC-related long-term displacement rates are low, based on previous work that found that, even for unusually strong TCs (Category 3 or greater at landfall), outward migration increases on average by only 6.85% in the year following the storms (Ouattara and Strobl, 2014).

## S.6 Selection of $K$

We wish to select a  $K$  value that preserves approximately 70% of the variance in the panel data matrix for all TCs and all outcomes. 70% is chosen because it represents a compromise between retaining variability necessary for accurate predictions, while not overfitting to the data. To explore the choice of  $K$  that best satisfies this criterion, we conduct exploratory principal component analyses (PCA) on the panel data matrices. Specifically, we remove the final column of the panel data matrix for each TC and outcome (because it contains missing values which are not permitted in PCA), and we implement PCA on each resulting matrix. The scree plots showing the percent of variance explained by each principal component (for each panel data matrix) are shown in Figure S.3. On average across TCs, the first four principal components explain 63% of the variance in mortality, 73% in respiratory hospitalizations, 70% in COPD hospitalizations, and 74% in CVD hospitalizations. Thus  $K = 4$  appears to be a reasonable choice to preserve around 70% of the variability in the panel data matrices. Moreover, as demonstrated by Figure S.3, each principal component beyond the fourth generally explains less than 10% of the variance in the panel data.

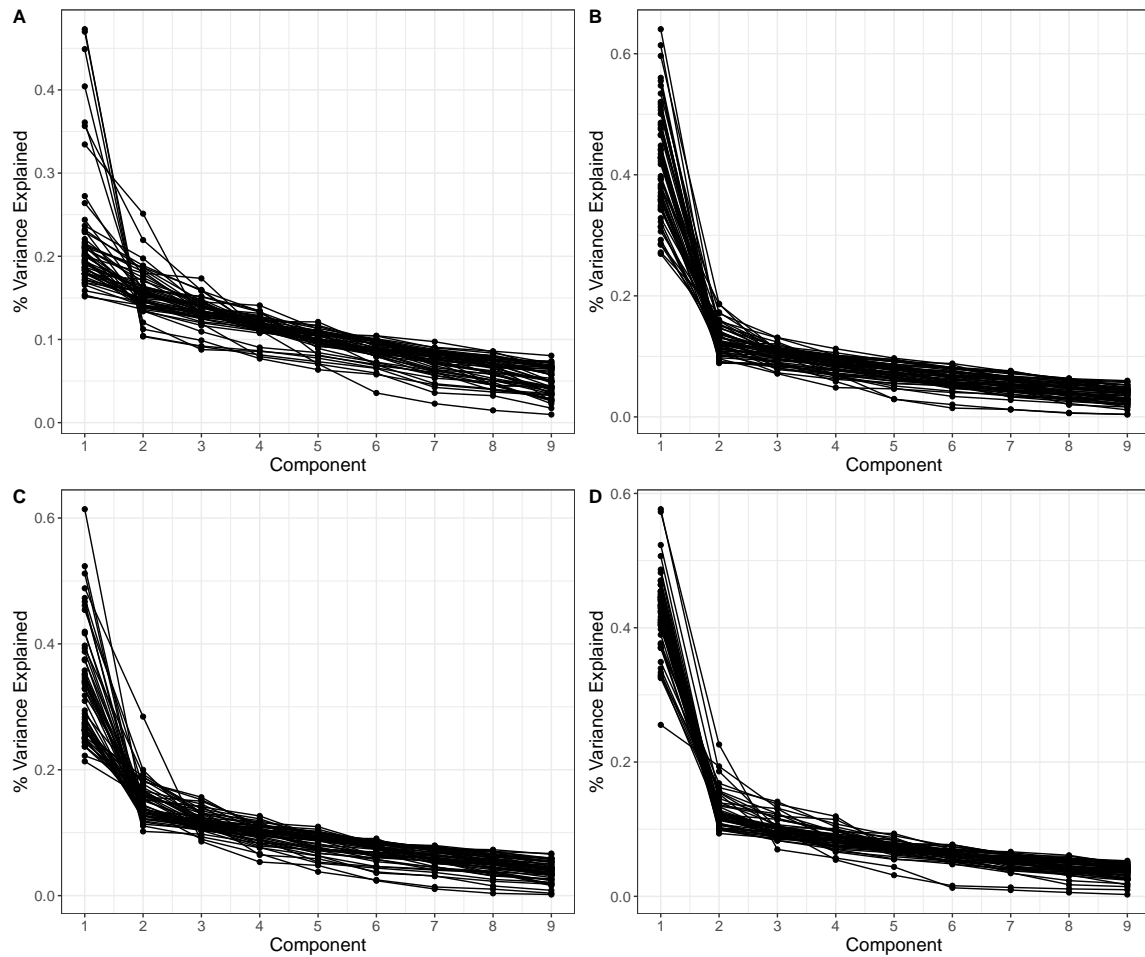


Figure S.3: Scree plots for PCA fit to the panel data matrix for each TC for mortality (A), respiratory hospitalizations (B), COPD hospitalizations (C), and CVD hospitalizations (D).

## S.7 Predictive model selection

Candidate predictive models are Bayesian additive regression trees (Chipman et al., 2010) (BART) and numerous variants of a linear regression model. In the regression models, we always include a restricted cubic spline on year to allow for flexible time trends in health effects of TCs. We consider regression models with (1) all additional predictors included as linear terms, (2) a restricted cubic spline on TC maximum sustained windspeed and all additional predictors included as linear terms, and (3) interactions between all predictors and a binary indicator of hurricane-speed winds (sustained windspeeds  $> 33\text{m/s}$ ). We test each predictive model candidate both with and without state included as a predictor.

To evaluate and compare predictive models, we fit them by plugging in the county-level excess rate point estimates as the outcomes (without passing their full posterior distributions into the predictive model). Using five-fold cross-validation, we compare out-of-sample predictive performance of these models. Root mean square error for each model is given in Table S.2. For most outcomes, we find similar predictive performance across models. Overall, we find the most consistently strong performance for the regression models with splines on windspeed, excluding state. Thus, for the primary predictive sub-model, we select the Bayesian linear model with a spline on windspeed, excluding state as a predictor. For interpretability, we also provide results from a linear regression model without the windspeed spline.

Table S.2: Root mean square error from 5-fold cross-validation for each considered predictive model.

|                              | Mortality    | Resp         | COPD         | CVD          |
|------------------------------|--------------|--------------|--------------|--------------|
| Linear with state            | 90.15        | 64.24        | 41.82        | 96.99        |
| Linear without state         | 89.96        | 64.34        | 42.08        | 95.84        |
| Spline with state            | 89.92        | <b>64.15</b> | 41.88        | 96.99        |
| Spline without state         | <b>89.59</b> | 64.25        | 42.14        | <b>95.83</b> |
| Linear, hurricane stratified | 92.15        | 64.57        | 42.41        | 96.04        |
| Spline, hurricane stratified | 92.17        | 64.57        | 42.45        | 96.05        |
| BART with state              | 90.85        | 64.28        | <b>41.53</b> | 95.85        |
| BART without state           | 101.36       | 64.26        | 41.97        | 96.07        |

## S.8 Sensitivity analyses

### S.8.1 Causal models

Because TC exposures are complex, our use of a binary TC exposure metric in the causal models could lead to some degree of exposure misclassification. In our models, we use as “controls” counties that are classified as unexposed and are within 150 miles of at least one exposed county. Because these controls counties lie near the path of the TC, it is likely that some of them received impacts. We anticipate that, if anything, including these counties as controls would lead to conservative results (i.e., treatment effects that are closer to the null). However, to evaluate the degree of influence this misclassification could have on our results, we fit causal models excluding from each TC’s model any control county that is adjacent to an exposed county. We expect that the counties nearest to exposed counties would be most likely to experience TC impacts. Figure S.4 compares the resulting county-level excess rate estimates with the estimates from our primary models. The estimates from the two models are highly clustered around the one-to-one line for all outcomes, with no clear systematic differences. This suggests that the causal models are robust to TC exposure misclassification.

Moreover, in the causal models, results could be sensitive to the specification of the number of latent factors,  $K$ . Thus, we compare the county-level excess rate estimates obtained when specifying  $K = \{3, 5\}$  to the estimates from our main model with  $K = 4$ . The comparison of the estimates from these models is shown in Figures S.5 and S.6. As in the previous sensitivity analysis, estimates from the models are highly clustered around the one-to-one line for all outcomes, with no clear systematic differences. This suggests that our results are robust to the specification of  $K$ .

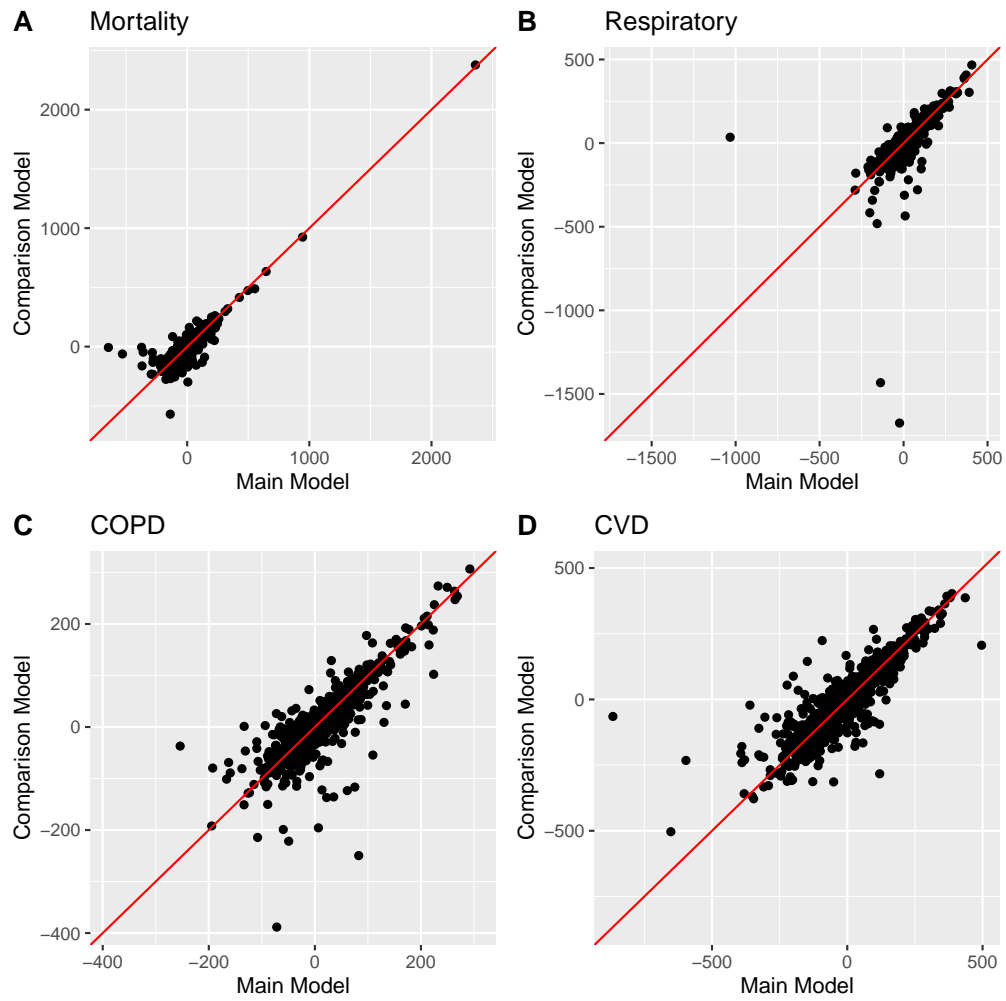


Figure S.4: County-level excess rate estimates from the main causal models compared to causal models with counties adjacent to TC-exposed counties removed.

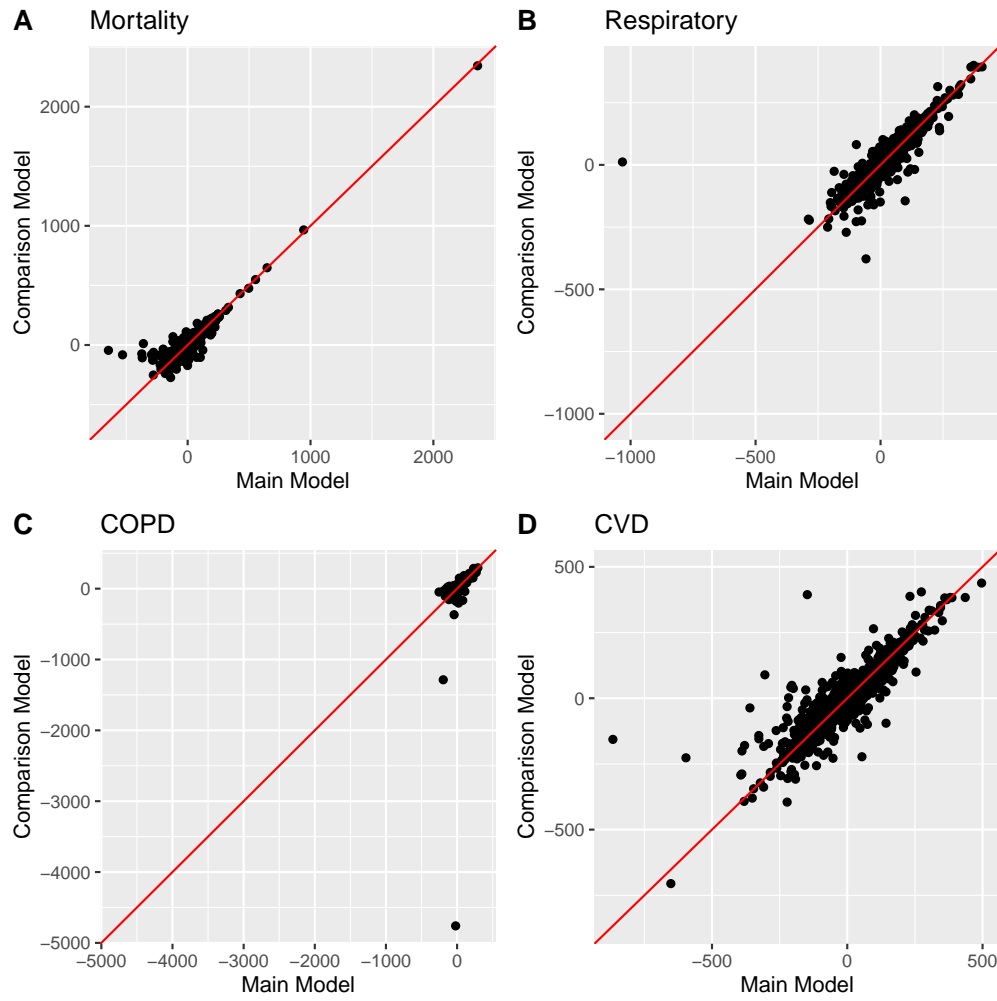


Figure S.5: County-level excess rate estimates from the main causal models ( $K = 4$ ) compared to causal models with  $K = 3$ .

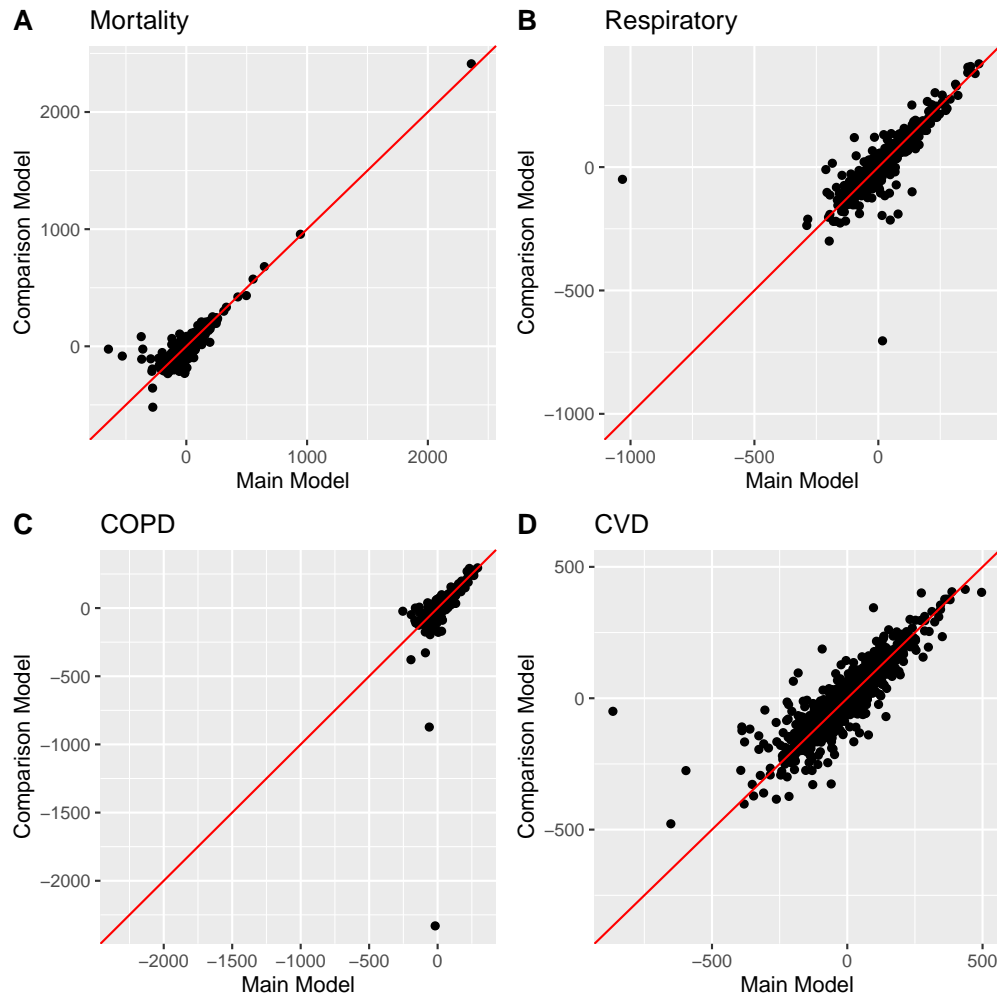


Figure S.6: County-level excess rate estimates from the main causal models ( $K = 4$ ) compared to causal models with  $K = 5$ .

### S.8.2 Predictive model

TCs can bring extreme rainfall amounts and flooding, and we hypothesize that these exposures may cause increases in some adverse health events. Currently, the `hurricaneexposedata` package contains TC rainfall data only through the year 2011. Due to the missing precipitation data for later years, we do not include this variable in our main predictive models, but here, as an additional sensitivity analysis, we fit the predictive models only using TCs in years 2011 and prior with precipitation as a predictor. As in the primary models, we fit regression models excluding state indicators but including all other predictors, with restricted cubic splines on windspeed and year. We also include a restricted cubic spline on county-level cumulative TC precipitation, measured over a four-day window starting two days prior to the storm's closest approach to the county. The precipitation splines from the fully modularized models are shown in Figure S.7. After adjusting for all the other predictors, there appears to be weak or no effect of precipitation on any of the health outcomes evaluated here. Thus, the inference and predictions from our model are unlikely to be sensitive to the inclusion of precipitation information.

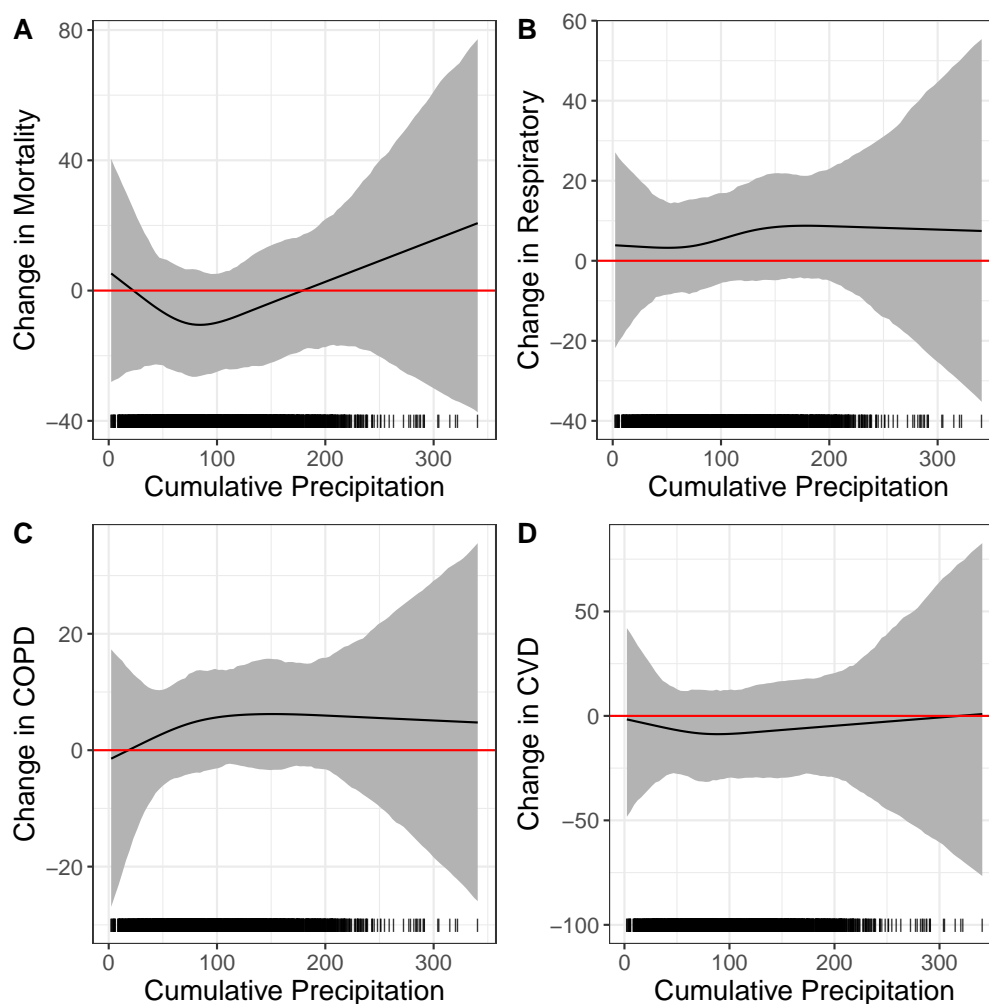


Figure S.7: Relationship between cumulative precipitation and excess rate per 100,000 of mortality (A), respiratory hospitalizations (B), COPD hospitalizations (C), and CVD hospitalizations (D).



## S.9 Additional tables and figures

Table S.3: Definition of estimands.  $s = \{1, \dots, S\}$  indexes TCs and  $i \in W_s$  indexes treated counties for TC  $s$ .

| Name                           | Definition  | Formula  |
|--------------------------------|---|--|
| Individual excess events (IEE) | County-level excess events attributable to a single TC $s$ over the treatment period                              | $\theta_{si} = \sum_{t \geq T_0} [Y_{sit}(1) - Y_{sit}(0)]$  |
| Individual excess rate         | County-level excess event rate (per 100,000 population) attributable to a single TC $s$ over the treatment period | $\theta_{si}^* = 100000 \times (\theta_{si}/p_{iT})$   |
| TC-specific excess events      | Cumulative excess events summed across all counties impacted by a single TC $s$                                   | $\sum_{i \in W_s} \theta_{si}$   |
| TC-specific excess rate        | Excess event rate (per 100,000 population) across all counties impacted by a single TC $s$                        | $100000 \times (\sum_{i \in W_s} p_{iT})^{-1} \sum_{i \in W_s} \theta_{si}$  |
| Total excess events (TEE)      | Cumulative TC-attributable excess events summed over all TCs and counties in the study                            | $TEE = \sum_{s=1}^S \sum_{i \in W_s} \theta_{si}$  |
| Average excess rate (AER)      | Average of the TC-attributable excess rates across all county-level TC exposures in the study                     | $AER = \frac{1}{N_{total}} \sum_{s=1}^S \sum_{i \in W_s} \theta_{si}^*$<br>$N_{total} = \sum_{s=1}^S  W_s $ is the total number of county-level TC exposures in our analyses |

Table S.4: Name and year of each TC included in the study, the number of treated and control counties for the TC, and the rates (per 100,000) of each health outcome in Medicare in the treated and control counties during the 140 day period surrounding the TC.

| TC             | N Trt | N Ctl | Mort Trt | Mort Ctl | Resp Trt | Resp Ctl | COPD Trt | COPD Ctl | CVD Trt | CVD Ctl |
|----------------|-------|-------|----------|----------|----------|----------|----------|----------|---------|---------|
| Alberto-2006   | 21    | 130   | 2036     | 1901     | 1361     | 1088     | 494      | 413      | 3210    | 2779    |
| Alex-2004      | 18    | 86    | 1828     | 1858     | 1052     | 909      | 380      | 331      | 2882    | 2868    |
| Allison-2001   | 22    | 143   | 2161     | 2209     | 1483     | 2050     | 584      | 743      | 3433    | 3832    |
| Ana-2015       | 3     | 52    | 1476     | 1751     | 800      | 875      | 369      | 355      | 1838    | 1971    |
| Andrea-2013    | 80    | 223   | 1718     | 1667     | 899      | 850      | 373      | 356      | 2059    | 1897    |
| Arlene-2005    | 4     | 61    | 1871     | 2189     | 1472     | 1805     | 561      | 669      | 3010    | 3288    |
| Arthur-2014    | 45    | 113   | 1642     | 1541     | 618      | 607      | 248      | 251      | 1864    | 1579    |
| Barry-2001     | 18    | 59    | 1971     | 2099     | 1412     | 1397     | 556      | 554      | 3418    | 3552    |
| Barry-2007     | 8     | 73    | 1778     | 1841     | 729      | 947      | 272      | 370      | 2187    | 2616    |
| Beryl-2012     | 22    | 114   | 1638     | 1664     | 853      | 897      | 366      | 409      | 1996    | 2118    |
| Bill-2003      | 16    | 77    | 2139     | 2056     | 1400     | 1581     | 546      | 554      | 3786    | 3495    |
| Bill-2015      | 9     | 47    | 1793     | 1585     | 929      | 852      | 343      | 322      | 1877    | 1708    |
| Bret-1999      | 15    | 28    | 1611     | 1903     | 1015     | 995      | 386      | 362      | 3101    | 2863    |
| Charley-2004   | 76    | 120   | 1758     | 1801     | 849      | 918      | 341      | 333      | 2980    | 2804    |
| Cindy-2005     | 13    | 78    | 2330     | 2004     | 1357     | 1562     | 489      | 560      | 3247    | 3086    |
| Claudette-2003 | 36    | 41    | 1914     | 1866     | 1163     | 1433     | 399      | 531      | 3018    | 3370    |
| Claudette-2009 | 3     | 53    | 1700     | 1787     | 1056     | 996      | 489      | 464      | 2713    | 2535    |
| Dennis-1999    | 23    | 94    | 1792     | 1864     | 988      | 904      | 427      | 356      | 3058    | 2859    |
| Dennis-2005    | 35    | 81    | 1990     | 2105     | 1452     | 1360     | 541      | 506      | 3254    | 2858    |
| Dolly-2008     | 13    | 22    | 1617     | 1659     | 1123     | 783      | 429      | 290      | 2536    | 2088    |
| Edouard-2008   | 10    | 72    | 2025     | 1767     | 1216     | 966      | 502      | 400      | 2565    | 2435    |
| Ernesto-2006   | 72    | 192   | 1698     | 1734     | 787      | 789      | 307      | 296      | 2494    | 2653    |
| Fay-2002       | 2     | 47    | 2047     | 1853     | 796      | 995      | 189      | 381      | 3541    | 3010    |
| Fay-2008       | 52    | 50    | 1634     | 1794     | 763      | 884      | 354      | 409      | 2321    | 2370    |
| Floyd-1999     | 142   | 156   | 1765     | 1824     | 904      | 890      | 315      | 325      | 2776    | 2913    |
| Frances-2004   | 50    | 39    | 1734     | 1843     | 842      | 974      | 352      | 391      | 2960    | 3178    |
| Gabrielle-2001 | 23    | 26    | 1802     | 1827     | 851      | 930      | 349      | 388      | 3073    | 3256    |
| Gabrielle-2007 | 6     | 71    | 1696     | 1770     | 763      | 715      | 360      | 273      | 2292    | 2413    |
| Gaston-2004    | 25    | 116   | 1761     | 1788     | 879      | 819      | 336      | 281      | 2855    | 2701    |
| Gordon-2000    | 12    | 63    | 1862     | 1775     | 817      | 826      | 371      | 343      | 3018    | 3111    |
| Gustav-2008    | 48    | 77    | 1844     | 1761     | 1062     | 914      | 431      | 392      | 2811    | 2341    |
| Hanna-2002     | 2     | 74    | 1871     | 1973     | 960      | 1198     | 388      | 478      | 3397    | 3339    |
| Hanna-2008     | 127   | 163   | 1660     | 1681     | 763      | 759      | 325      | 321      | 2470    | 2202    |
| Harvey-1999    | 3     | 20    | 1876     | 1739     | 1309     | 823      | 535      | 334      | 3300    | 2950    |
| Helene-2000    | 14    | 96    | 1988     | 1913     | 1089     | 960      | 418      | 381      | 3139    | 2983    |
| Hermine-2010   | 13    | 30    | 1515     | 1599     | 891      | 742      | 369      | 295      | 2063    | 1897    |
| Humberto-2007  | 31    | 81    | 1766     | 1838     | 942      | 956      | 334      | 329      | 2490    | 2580    |
| Ike-2008       | 215   | 64    | 1782     | 1756     | 924      | 874      | 411      | 350      | 2471    | 2414    |
| Irene-1999     | 28    | 125   | 1777     | 1820     | 1015     | 875      | 411      | 360      | 3119    | 2889    |
| Irene-2011     | 146   | 146   | 1622     | 1623     | 793      | 755      | 329      | 313      | 2046    | 1884    |
| Isaac-2012     | 41    | 70    | 1769     | 1785     | 888      | 936      | 343      | 393      | 2068    | 2062    |
| Isabel-2003    | 135   | 86    | 1857     | 1890     | 1008     | 1036     | 362      | 378      | 2778    | 3079    |
| Isidore-2002   | 25    | 80    | 2025     | 1981     | 1200     | 1221     | 486      | 463      | 3627    | 3291    |
| Ivan-2004      | 48    | 72    | 1867     | 1959     | 1108     | 989      | 472      | 376      | 3428    | 3018    |
| Jeanne-2004    | 45    | 35    | 1731     | 1830     | 834      | 874      | 352      | 346      | 2977    | 3020    |
| Katrina-2005   | 78    | 72    | 1875     | 1781     | 957      | 902      | 370      | 338      | 2726    | 2856    |
| Lee-2011       | 30    | 91    | 1769     | 1785     | 841      | 969      | 372      | 406      | 2159    | 2136    |
| Lili-2002      | 34    | 86    | 1982     | 1962     | 1248     | 1148     | 452      | 447      | 3565    | 3228    |
| Ophelia-2005   | 23    | 112   | 1687     | 1728     | 872      | 819      | 344      | 307      | 2782    | 2629    |
| Rita-2005      | 40    | 89    | 1803     | 1823     | 989      | 866      | 381      | 322      | 2760    | 2687    |
| Sandy-2012     | 105   | 121   | 1606     | 1671     | 683      | 718      | 288      | 297      | 1911    | 1843    |
| Tammy-2005     | 12    | 52    | 1789     | 1734     | 873      | 793      | 313      | 315      | 2847    | 2697    |
| Wilma-2005     | 18    | 21    | 1689     | 1735     | 770      | 767      | 305      | 310      | 2603    | 2714    |

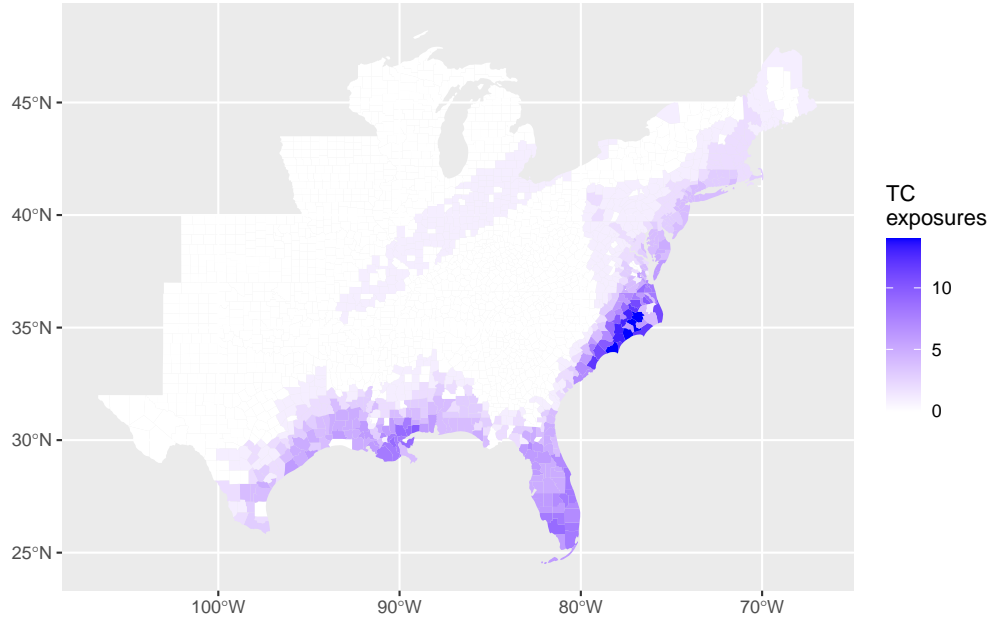


Figure S.8: Number of Atlantic Basin TC exposures included in our analyses (by county), 1999-2015.

Table S.5: Predictive model coefficient posterior means (95% CIs) from models with a natural cubic spline on sustained windspeed and year, not adjusted for state. Variable names with suffix *\_s* are components of a restricted cubic spline basis for the variable.

|                    | Mortality                 | Resp                    | COPD                     | CVD                       |
|--------------------|---------------------------|-------------------------|--------------------------|---------------------------|
| (Intercept)        | -115.89 (-378.81, 107.09) | 39.13 (-113.1, 198.02)  | 18.07 (-117.22, 137.78)  | -45.97 (-333.02, 243.32)  |
| vmax_sust_s1       | 4.34 (-7.09, 17.48)       | -0.97 (-8.93, 6.6)      | 0.43 (-5.6, 6.75)        | 2.38 (-11.82, 15.2)       |
| vmax_sust_s2       | -92.36 (-248.23, 37.85)   | -6.37 (-97.13, 87.88)   | 7.56 (-69.23, 80.78)     | -41.31 (-194, 129.42)     |
| vmax_sust_s3       | 181.19 (-46.76, 449.3)    | 19.6 (-143.67, 180.82)  | -12.29 (-140.88, 124.59) | 78.09 (-221.95, 345.87)   |
| poverty            | 35.26 (-149.01, 206.88)   | 114.78 (-22.65, 244.98) | 20.54 (-79.69, 119.58)   | -121.81 (-375.06, 110.56) |
| white_pct          | 14.23 (-38.78, 64.42)     | -24.13 (-62.07, 12.89)  | -32.12 (-61.3, -4.57)    | 17.56 (-51.28, 89.96)     |
| owner_occupied     | -16.78 (-115.76, 84.09)   | 17.94 (-60.87, 89.38)   | 38.48 (-20.04, 95.68)    | -91.02 (-239.35, 49.81)   |
| age_pct_65_plus    | -165.94 (-486.81, 139.45) | 7.66 (-241.24, 225.26)  | 36.44 (-141.45, 213.65)  | -95.8 (-514.39, 300.21)   |
| median_age         | 1.26 (-2.29, 5.05)        | 0.02 (-2.27, 2.52)      | -0.49 (-2.4, 1.57)       | 1.72 (-2.57, 6.62)        |
| population_density | -0.58 (-7.57, 6.61)       | 0.02 (-5.34, 4.98)      | 0.82 (-3.13, 4.8)        | -0.97 (-9.88, 7.72)       |
| median_house_value | 2.83 (-7.67, 12.33)       | 0.62 (-5.89, 7.82)      | -0.38 (-6.05, 5.11)      | -5.61 (-18.46, 7.29)      |
| no_grad            | 14.72 (-137.05, 154.17)   | -62.79 (-167.04, 40.83) | -25.48 (-106.23, 58.74)  | 36.94 (-143.44, 207.96)   |
| year_s1            | -1.78 (-17.02, 14.35)     | 6.97 (-4.91, 19.73)     | 6.64 (-2.85, 15.56)      | -2.08 (-23.65, 17.19)     |
| year_s2            | -2.92 (-21.43, 13.73)     | -11.03 (-24.57, 1.7)    | -8.55 (-18.28, 1.86)     | 4.73 (-16.43, 27.76)      |
| exposure           | 1.19 (-0.78, 3.25)        | -1.61 (-3.02, -0.17)    | -1.29 (-2.35, -0.24)     | 0.17 (-2.12, 2.84)        |
| sust_dur           | 0.01 (-0.02, 0.05)        | 0.03 (0.01, 0.06)       | 0 (-0.02, 0.02)          | -0.01 (-0.05, 0.04)       |
| cc1                | -2.37 (-16.09, 12.75)     | -1.24 (-11.75, 9.38)    | -2.17 (-9.82, 5.43)      | 8.19 (-9.89, 27.44)       |

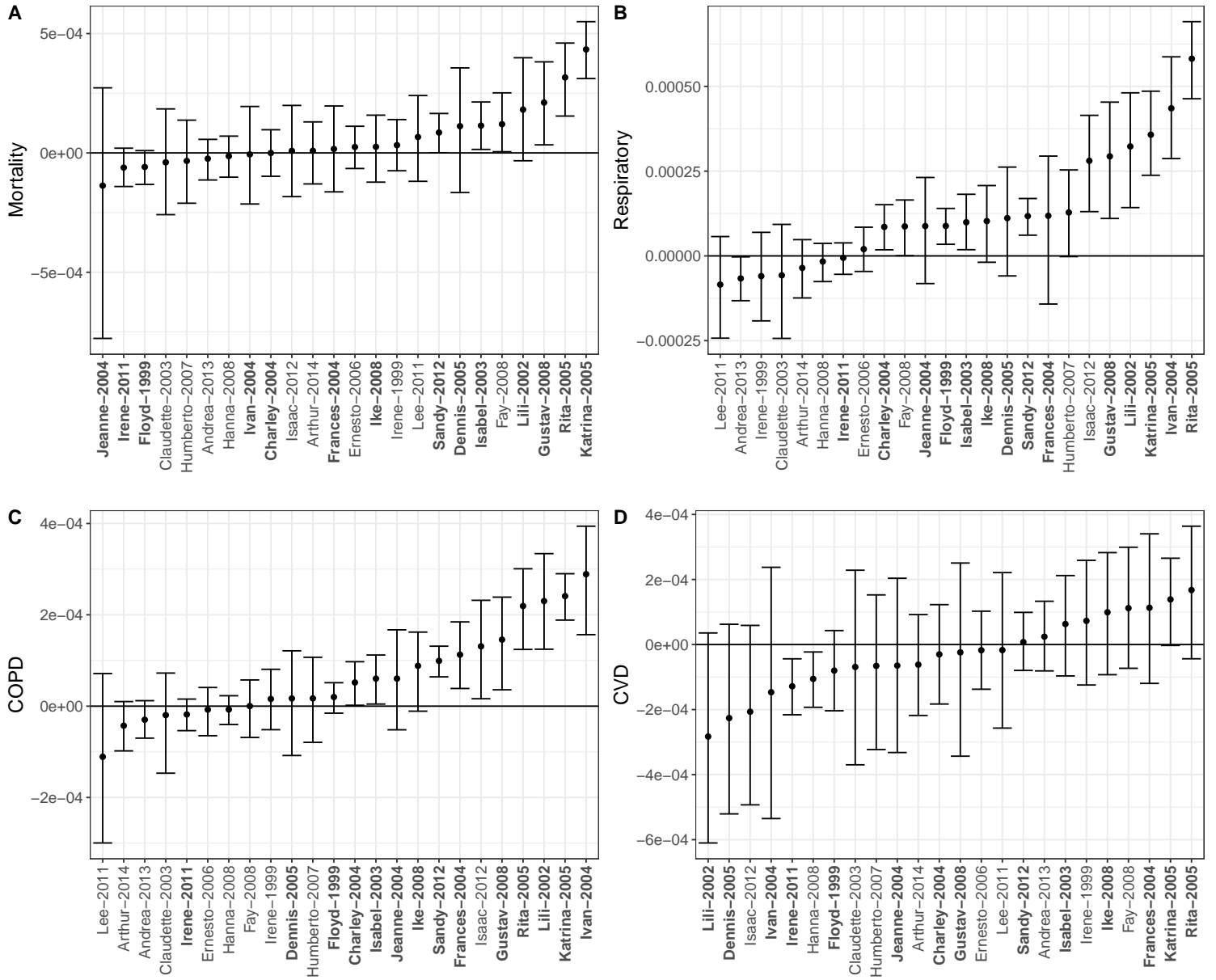


Figure S.9: TC-specific excess rate estimates and 95% predictive intervals for mortality (A), respiratory hospitalizations (B), COPD hospitalizations (C), and CVD hospitalizations (D) for TCs that impacted  $> 25$  counties. The TC-specific excess rate is the rate of excess events across the total population impacted by the TC. Bolded TC labels indicate storm names that were subsequently retired—retirement occurs when a TC is so destructive that re-using the name is considered to be insensitive (National Hurricane Center, 2020).

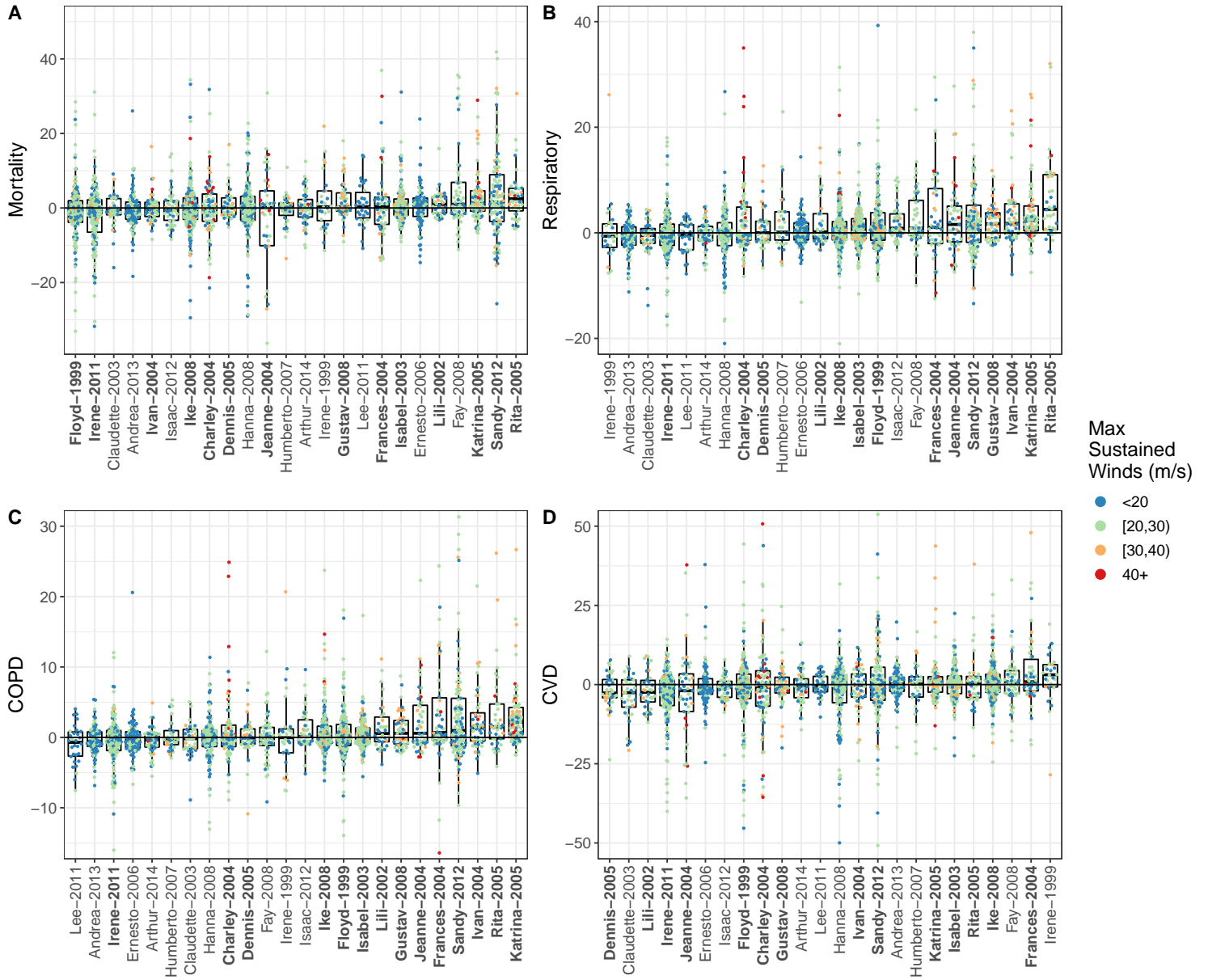


Figure S.10: County-level individual excess events (IEE) estimates for mortality (A), respiratory hospitalizations (B), COPD hospitalizations (C), and CVD hospitalizations (D) for TCs that impacted > 25 counties. The IEE is the estimated number of excess events in the county due to the TC. Distant outliers are cropped out for readability. Bolded TC labels indicate storm names that were subsequently retired—retirement occurs when a TC is so destructive that re-using the name is considered to be insensitive (National Hurricane Center, 2020).

Table S.6: Predictive model coefficient posterior means (95% CIs) from models linear models (spline term only on the year variable), not adjusted for state. Variable names with suffix `_s` are components of a restricted cubic spline basis for the variable.

|                    | Morality                  | Resp                    | COPD                    | CVD                      |
|--------------------|---------------------------|-------------------------|-------------------------|--------------------------|
| (Intercept)        | -101.38 (-216.44, 8.75)   | -6.18 (-84.45, 74.71)   | 0.89 (-57.79, 60.08)    | -19.05 (-155.97, 118.74) |
| vmax_sust          | 3.21 (1.59, 5.09)         | 1.39 (0.16, 2.59)       | 1.36 (0.42, 2.28)       | 0.84 (-1.24, 3.08)       |
| sust_dur           | -0.01 (-0.05, 0.02)       | 0.02 (0, 0.04)          | 0 (-0.01, 0.02)         | -0.01 (-0.05, 0.03)      |
| exposure           | 1.36 (-0.64, 3.3)         | -1.59 (-2.96, -0.27)    | -1.28 (-2.37, -0.2)     | 0.27 (-2.08, 2.76)       |
| poverty            | 48.39 (-135.71, 228.03)   | 118.2 (-15.32, 241.09)  | 22.36 (-82.63, 125.13)  | -116.76 (-366.75, 110.8) |
| white_pct          | 12.55 (-39.29, 64.74)     | -25.91 (-66.17, 10.07)  | -32.12 (-61.68, -3.08)  | 17.14 (-50.02, 88.44)    |
| owner_occupied     | -4.82 (-110.78, 98.17)    | 21.51 (-50.72, 97.63)   | 38.45 (-16.56, 96.45)   | -90.14 (-233.67, 52.13)  |
| age_pct_65_plus    | -123.03 (-446.07, 210.72) | 27.06 (-207.2, 253.55)  | 44.02 (-133.55, 217.4)  | -91.54 (-519.72, 298.64) |
| median_age         | 0.78 (-2.99, 4.59)        | -0.19 (-2.63, 2.31)     | -0.53 (-2.54, 1.49)     | 1.68 (-2.75, 6.38)       |
| population_density | -1.1 (-7.94, 5.71)        | -0.36 (-5.12, 5.01)     | 0.75 (-2.95, 4.46)      | -1.22 (-10.09, 7.51)     |
| median_house_value | 3.64 (-6.72, 13.2)        | 0.84 (-6.38, 7.94)      | -0.19 (-5.42, 5.52)     | -5.52 (-18.1, 7.11)      |
| no_grad            | 19.87 (-126.09, 162.17)   | -57.28 (-163.61, 47.03) | -26.03 (-108.24, 52.87) | 37.35 (-136.49, 216.22)  |
| year_s1            | -0.85 (-17.39, 15.05)     | 7.34 (-3.76, 18.99)     | 6.72 (-3.06, 15.65)     | -1.08 (-21.94, 19.25)    |
| year_s2            | -3.84 (-21.69, 15.86)     | -11.46 (-24.17, 1.48)   | -8.8 (-18.86, 1.73)     | 3.62 (-20.64, 27.44)     |
| cc1                | -1.23 (-16.32, 13.4)      | -1.05 (-11.84, 9.45)    | -2.47 (-10.36, 5.16)    | 8.5 (-9.28, 27)          |

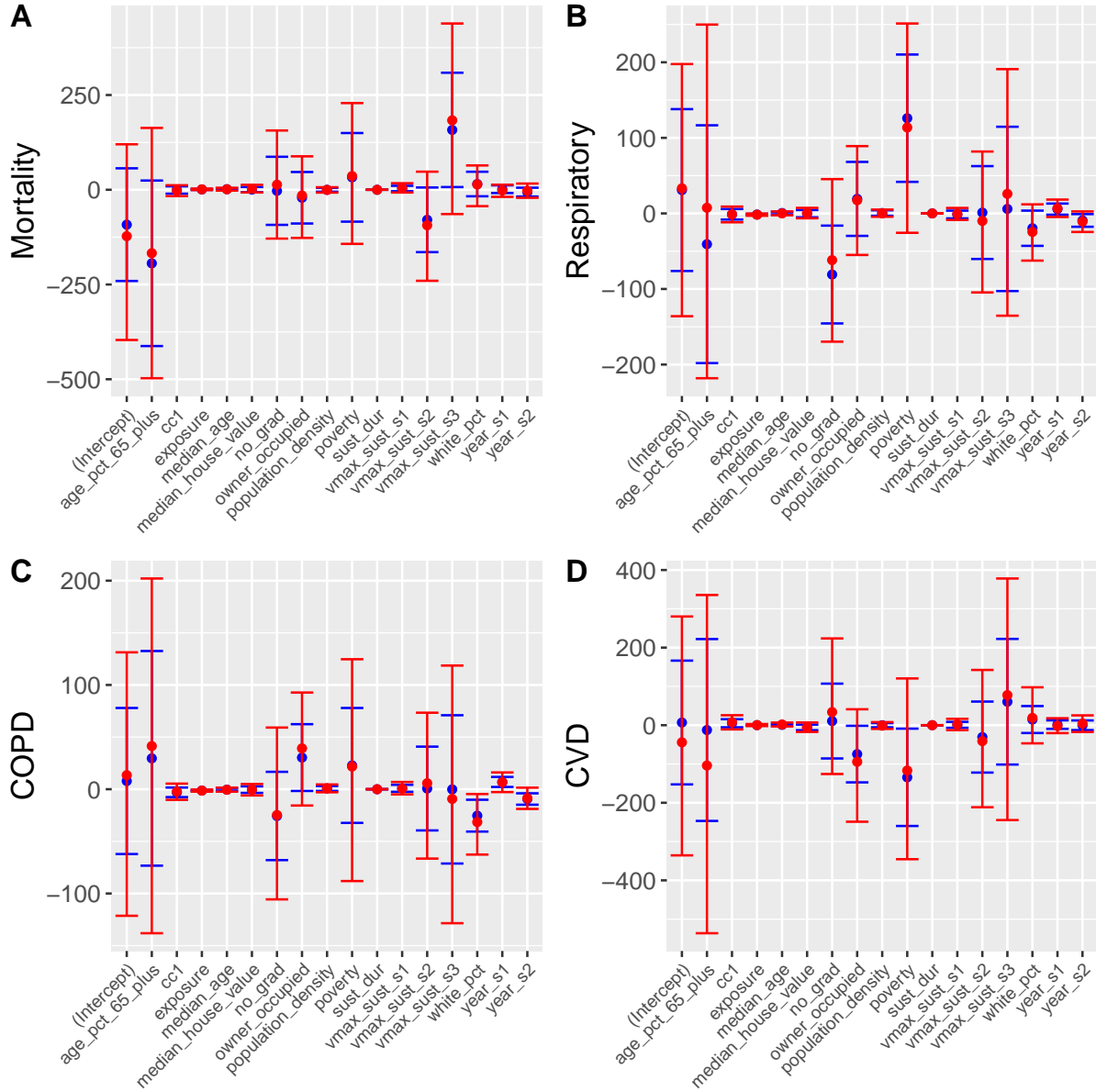


Figure S.11: Point estimates and 95% CIs from predictive models for each outcome that do propagate uncertainty from the causal models (red) and do not propagate uncertainty (blue).

## Supplemental references

- Anderson, B., A. Schumacher, W. Crosson, M. Al-Hamdan, M. Yan, J. Ferreri, Z. Chen, S. Quiring, and S. Guikema (2017). *hurricaneexposedata: Data Characterizing Exposure to Hurricanes in United States Counties*. R package version 0.0.2.
- Anderson, B., M. Yan, J. Ferreri, W. Crosson, M. Al-Hamdan, A. Schumacher, and D. Eddelbuettel (2019). *hurricaneexposure: Explore and Map County-Level Hurricane Exposure in the United States*. R package version 0.1.0.
- Anderson, G. B., J. Ferreri, M. Al-Hamdan, W. Crosson, A. Schumacher, S. Guikema, S. Quiring, D. Eddelbuettel, M. Yan, and R. D. Peng (2020). Assessing United States county-level exposure for research on tropical cyclones and human health. *In press, Environmental Health Perspectives*.
- Chipman, H. A., E. I. George, R. E. McCulloch, et al. (2010). Bart: Bayesian additive regression trees. *The Annals of Applied Statistics* 4(1), 266–298.
- Deryugina, T. and D. Molitor (2018). Does when you die depend on where you live? evidence from hurricane katrina. Technical report, National Bureau of Economic Research.
- Gopalan, P. K., L. Charlin, and D. Blei (2014). Content-based recommendations with Poisson factorization. In *Advances in Neural Information Processing Systems*, pp. 3176–3184.
- Kuo, K.-L. and Y. J. Wang (2018). Simulating conditionally specified models. *Journal of Multivariate Analysis* 167, 171–180.
- Lim, Y. J. and Y. W. Teh (2007). Variational Bayesian approach to movie rating prediction. In *Proceedings of KDD cup and workshop*, Volume 7, pp. 15–21. Citeseer.
- Meng, X.-L. (1994). Multiple-imputation inferences with uncongenial sources of input. *Statistical Science*, 538–558.
- National Hurricane Center (2020 (accessed October 14, 2020)). *Tropical Cyclone Naming History and Retired Names*.
- Ouattara, B. and E. Strobl (2014). Hurricane strikes and local migration in us coastal counties. *Economics Letters* 124(1), 17–20.
- Pang, X., L. Liu, and Y. Xu (2020). A Bayesian alternative to synthetic control for comparative case studies. *Available at SSRN*.
- Rubin, D. B. (1980). Randomization analysis of experimental data: The fisher randomization test comment. *Journal of the American Statistical Association* 75(371), 591–593.
- Rubin, D. B. (2003). Nested multiple imputation of nmes via partially incompatible mcmc. *Statistica Neerlandica* 57(1), 3–18.
- Rui, H. and D. Mocko (2014). Readme Document for North America Land Data Assimilation System Phase 2 (NLDAS-2) Products. *Greenbelt, Maryland*.
- Salakhutdinov, R. and A. Mnih (2008). Bayesian probabilistic matrix factorization using Markov chain Monte Carlo. In *Proceedings of the 25th international conference on Machine learning*, pp. 880–887.
- Schafer, J. L. (2003). Multiple imputation in multivariate problems when the imputation and analysis models differ. *Statistica Neerlandica* 57(1), 19–35.
- Stan Development Team (2020). RStan: the R interface to Stan. R package version 2.19.3.



- Tanaka, M. (2019). Bayesian matrix completion approach to causal inference with panel data. *arXiv preprint arXiv:1911.01287*.
- Van Buuren, S. (2007). Multiple imputation of discrete and continuous data by fully conditional specification. *Statistical methods in medical research* 16(3), 219–242.
- Van Buuren, S., J. P. Brand, C. G. Groothuis-Oudshoorn, and D. B. Rubin (2006). Fully conditional specification in multivariate imputation. *Journal of statistical computation and simulation* 76(12), 1049–1064.
- Yan, M., A. Wilson, F. Dominici, Y. Wang, M. Al-Hamdan, W. Crosson, A. Schumacher, S. Guikema, S. Magzamen, J. L. Peel, R. D. Peng, and G. B. Anderson (2020). Tropical cyclone exposures and risks of emergency Medicare hospital admission for cardiorespiratory diseases in 175 urban United States counties, 1999–2010. *In press, Epidemiology*.
- Yang, L., J. Fang, H. Duan, H. Li, and B. Zeng (2018). Fast low-rank Bayesian matrix completion with hierarchical Gaussian prior models. *IEEE Transactions on Signal Processing* 66(11), 2804–2817.